BRL-TR-2999

④

TECHNICAL REPORT BRL-TR-2999

BRL

ELECTROTHERMAL GUNS--A THEORETICAL INVESTIGATION OF FACTORS FOR OPTIMAL PERFORMANCE

WILLIAM OBERLE

JUNE 1989

U.S. ARMY LABORATORY COMMAND

BALLISTIC RESEARCH LABORATORY
ABERDEEN PROVING GROUND, MARYLAND

DESTRUCTION NOTICE

UNCLASSIFIED

SECURITY CLASSIFICATION OF THIS PAGE

REPORT DOCUMENTATION PAGE

Form Approved OMB No. 0704-0188

1a. REPORT SECURITY CLASSIFICATION Unclassified	1b. RESTRICTIVE MARKINGS
2a. SECURITY CLASSIFICATION AUTHORITY	3. DISTRIBUTION / AVAILABILITY OF REPORT Approved for Public Release; Distribution Unlimited.
2b. DECLASSIFICATION / DOWNGRADING SCHEDULE	
4. PERFORMING ORGANIZATION REPORT NUMBER(S) BRL-TR-2999	5. MONITORING ORGANIZATION REPORT NUMBER(S)
6a. NAME OF PERFORMING ORGANIZATION US Army Ballistic Rsch Lab	6b. OFFICE SYMBOL *(If applicable)* SLCBR-IB
7a. NAME OF MONITORING ORGANIZATION	
6c. ADDRESS *(City, State, and ZIP Code)* Aberdeen Proving Ground, MD 21005-5066	7b. ADDRESS *(City, State, and ZIP Code)*
8a. NAME OF FUNDING / SPONSORING ORGANIZATION	8b. OFFICE SYMBOL *(If applicable)*
9. PROCUREMENT INSTRUMENT IDENTIFICATION NUMBER	
8c. ADDRESS *(City, State, and ZIP Code)*	10. SOURCE OF FUNDING NUMBERS

PROGRAM ELEMENT NO.	PROJECT NO.	TASK NO.	WORK UNIT ACCESSION NO.

11. TITLE *(Include Security Classification)*
ELECTROTHERMAL GUNS - A THEORETICAL INVESTIGATION OF FACTORS FOR OPTIMAL PERFORMANCE

12. PERSONAL AUTHOR(S)
Oberle, William F.

13a. TYPE OF REPORT	13b. TIME COVERED	14. DATE OF REPORT *(Year, Month, Day)*	15. PAGE COUNT
TR	FROM ______ TO ______		

16. SUPPLEMENTARY NOTATION

17. COSATI CODES			18. SUBJECT TERMS *(Continue on reverse if necessary and identify by block number)*
FIELD	GROUP	SUB-GROUP	Ballistics Electrothermal Gun Plasma Endothermic/Exothermic Working Fluids Capillary

19. ABSTRACT *(Continue on reverse if necessary and identify by block number)*

The electrothermal (ET) gun or electrothermal accelerator is an advanced propulsion concept in which an electrically generated high pressure and temperature plasma interacts with a carefully chosen working fluid to produce the necessary gases to accelerate the projectile. In theory the combustion process is completely controlled by the electrical power input used to generate and sustain the plasma. Thus, constant breech pressure and resulting optimal velocity should be obtainable by tailoring the power input for a given working fluid. Additionally, selecting working fluids which result in low molecular weight gases reduces the energy expended in accelerating the gases.

SEE CONTINUATION OF ABSTRACT ON REVERSE

20. DISTRIBUTION / AVAILABILITY OF ABSTRACT ☒ UNCLASSIFIED/UNLIMITED ☐ SAME AS RPT. ☐ DTIC USERS	21. ABSTRACT SECURITY CLASSIFICATION Unclassified	
22a. NAME OF RESPONSIBLE INDIVIDUAL William F. Oberle	22b. TELEPHONE *(Include Area Code)* (301) 278-6200	22c. OFFICE SYMBOL SLCBR-IB-B

DD Form 1473, JUN 86 *Previous editions are obsolete.* SECURITY CLASSIFICATION OF THIS PAGE

19. ABSTRACT (Con't)

In this report, using an appropriately modified interior ballistic code, several aspects of the electrothermal gun process and potential performance are investigated. ~~First,~~ conditions required of the electrical input and working fluid necessary to achieve the ideal constant breech pressure and optimal velocity are considered. Secondly, the sensitivity of ballistic performance and gas temperature for the electrothermal process is determined for perturbations in several factors felt to be critical to ET performance. Finally, differences arising from using non-energetic (endothermic) or energetic (exothermic) working fluid are addressed.

Results of the computer simulations indicate that an ET gun using either endothermic or exothermic working fluids can out perform conventional solid propulsion technology. The simulations indicate that the electrical power input required to drive the constant breech pressure is feasible given today's technology. However, mechanical requirements imposed on the reacting working fluids appear to be severe and may indicate difficulties with reproducibility. The parametric studies suggest that endothermic and exothermic working fluids respond differently to perturbations in the process. Finally, the study indicates that one of the critical factors in ET gun performance is reproducible plasma/working fluid interaction, impacting not only projectile velocity and pressure profiles, but more significantly, gas temperature.

ACKNOWLEDGMENT

The author would like to thank G. Wren and K. White for their helpful comments in the preparation of this report.

Table of Contents

List of Figures

List of Tables

I. INTRODUCTION

The electrothermal gun (ET gun) or electrothermal accelerator is a propulsion concept in which all or a portion of the energy used to accelerate the projectile is provided by an electrical source which is external to the gun breech. A complete ET gun system comprises four major components as shown in Figure 1. The first component consists of the necessary equipment for generation and storage of the required electrical power. A capillary is then required through which the electrical current (energy) flows creating a plasma of low mass but extremely high pressure and temperature. This plasma passes into the third component, the combustion chamber, in which the plasma interacts with a working fluid producing gases which accelerate the projectile through the final component of the system - the gun tube. A more detailed description of the ET propulsion process can be found in a separate paper.[1]

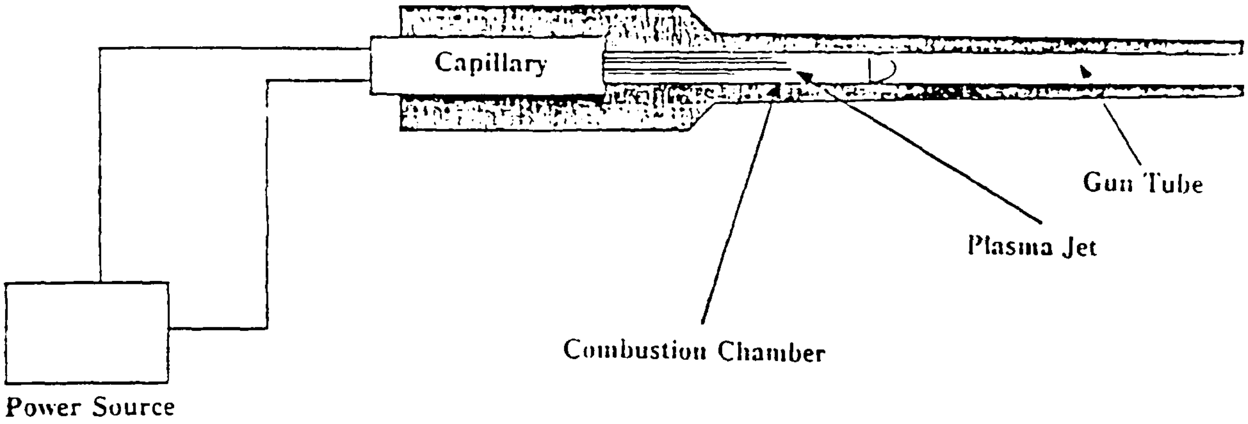

Figure 1: Schematic of Electrothermal Gun System

For a conventional solid propellant gun the constraining factors on performance in terms of muzzle velocity are chamber volume, gun strength, tube length and the combustion characteristics of the propellant. The gun chamber volume limits the amount of propellant and hence the total available energy; gun strength limits the pressures at which the gun can operate; while tube length effects the expansion ratio. Finally, the burning characteristics of the propellant determine the pressure profiles in the gun. An electrothermal gun is limited by similar constraints. Since an electrothermal gun relies on combustion gases to accelerate the projectile as in a conventional gun, gun strength and tube length will have the same limiting effect as in a solid propellant gun system. The rate and magnitude of the electrical energy input in combination with the thermochemical properties of the working fluid determine the pressurization rate and pressure profiles in the gun. However.

the ET gun differs from a conventional solid propellant gun in that chamber volume no longer represents a limitation on the total amount of energy available to the system. In theory, the electrical energy source is capable of providing unlimited energy. However, from a operational point of view, the maximum operating gun temperature limits the amount of energy which can be introduced into the system. In fact, thermal management for an ET gun may be more difficult than for conventional gun systems. For the conventional gun the overall temperature is bounded by the propellant flame temperature. Even if the rate of energy input increases due to an increase in the burning rate of the propellant, the maximum gun temperature is still limited to the flame temperature of the propellant. For an ET gun there is no upper limit on gas temperature. The temperature of the gases resulting from the interaction of the electrically created plasma and working fluid is an increasing function of the amount of electrical energy being transmitted to a unit mass of the working fluid.[6] Thus, temperature limitation results only through controlling the magnitude and rate of electrical energy input in combination with the mass and properties of the working fluid.

As described above, the magnitude and rate of electrical energy input, together with the properties of the working fluid, are the controlling factors in gun pressure profiles and overall gun temperatures. The purpose of this report is to investigate the electrical energy input, as described by the power versus time curve, and working fluid requirements necessary to obtain optimal performance (velocity) within a pressure constraint and determine the sensitivity of pressure, velocity and temperature to perturbations in these conditions. Specifically the objectives of this report are to:

a. investigate power curve requirements for a specific working fluid to obtain optimal performance.
b. investigate requirements of the working fluid - plasma interaction to meet the performance of (a).
c. investigate the sensitivity of pressure, velocity and temperature if the conditions for optimal performance are parametrically varied.
d. determine if the results and trends of parts (a) through (c) are dependent on the type of working fluid (endothermic vs. exothermic).
e. compare optimal electrothermal gun performance to that which can be obtained through solid propellant technology.

II. BACKGROUND

Currently, the BRL is involved in an experimental and a theoretical investigation of electrothermal propulsion. Experimental firings will initially employ a diagnostic fixture which has a moving boundary in a 14-mm bore diameter tube. This diameter was selected since a previous BRL experimental program in advanced propellant technology, for which a large data base of both experimental and computer simulation exists, utilized a similar 14 mm bore diameter gun.[2] In addition, projectile masses utilized in the simulations were selected based on this earlier experimental program. Using these parameters allow comparisons with the previous data base and provide information relevant to the current experimental effort. Exact details of the gun geometry and projectile mass are given in Table 1.

TABLE 1: Gun And Projectile Parameters Used For Computer Simulations

Gun Specifications:
Chamber Volume -- 97.108 cm^3
Chamber Length -- 15.875 cm^3
Chambrage -- Yes
Projectile Travel -- 145 cm
Bore Diameter -- 14 mm
Calibers of Travel -- 104
Expansion Ratio -- 3.3

Projectile Mass: 18 g

In addition to choosing a gun envelope for the study, it was necessary to select working fluids from a number of possible candidates. In an idealized electrothermal gun, the electrical power source provides all the energy for the gun. However, recent experimental efforts[3,4] have involved the use of mildly and highly exothermic working fluids. Therefore, in this study four working fluids which are representative of working fluids currently being used or contemplated for electrothermal propulsion are investigated. The working fluids include two non-energetic (endothermic), one mildly energetic (exothermic) and one which is highly energetic (exothermic). At present, it is planned that these or similar fluids will be used in the BRL experimental firings. A description, as well as thermochemical properties of the working fluids, are given in Table 2. First, however, the method of obtaining the values is briefly explained and terminology used in the table is defined

To compute the thermochemical properties of the working fluid/electrical energy combination the equilibrium thermodynamic computer code BLAKE[5] was utilized. Several guidelines were developed for selecting the proper thermochemical values for the working fluids. First, in performing the BLAKE calculations the electrical energy input was included as part of the working fluid so that the results would reflect the total energy available to do work on the projectile. Second, to provide the thermal management discussed in the introduction, the amount of electrical energy was adjusted so that the resulting theoretical temperature of the resulting gaseous mixture would be approximately 3450 K, the flame temperature of the solid propellant JA2. Finally, if the working fluid was a combination of several fluids, the mass ratio of the fluids was varied to obtain maximum impetus. Generally, the resulting mass ratios were not in stoichiometric balance. A detailed description of this process is included in a separate paper.[6]

Special terminology used in Table 2 is given below.

KJ of Electrical Energy (KJ Elec En.): The number of kilojoules of electrical energy included in the BLAKE calculation per gram of working fluid.

Effective Energy (Eff. En.): The total available energy per gram of working fluid predicted by BLAKE. This figure includes both electrical and chemical energy and is the measure of the energy available to do work.

Several entries in the Table 2 merit attention. First, molecular weight is that of the gas formed in the reaction. For the TiH_2/Al mixture at a temperature of 3450 K the predominate gas formed is hydrogen, hence, the low molecular weight of 2.33. Next is the effective energy of H_2O and $LiBH_4$. As can be observed in Table 2, the effective energy for these working fluids is less than the electrical energy which was added and, thus, these fluids are classified as non-energetic or endothermic for this study. The difference in energy, 1.769 kJ/g for H_2O and 1.85 kJ/g for $LiBH_4$, is the energy required to transition the working fluid to the gaseous state. This energy would not be available to perform work on the projectile unless the expansion ratio became infinite and the gases were allowed to condense. Thus, this energy is not included in the effective energy for the working fluid. The same is true of exothermic working fluids. However, since chemical energy is released for exothermic fluids the short fall in energy is not evident.

TABLE 2: Working Fluids And Their Properties

Working Fluids:

1. Water, H_2O;Endothermic (H2O)
2. $LiBH_4$ & H_2O in a 40/60 ratio; Endothermic (LiBH4)
3. TiH_2 & H_2O mixed with Al & H_2O in a 30/70 ratio
   Note: Both sub-mixtures, TiH_2 & H_2O and Al & H_2O were 50/50 mixtures which gave maximum impetus for each, however, the final 30/70 mixture was not optimized by BLAKE to provide maximum impetus.
   Mildly Exothermic (TiH2/Al)
4. Octane & Peroxide, C_8H_{18} & H_2O_2; Highly Exothermic (C8H18/H2O2)

Note: Throughout the remainder of this report the different working fluids are referenced by the expression in parenthesis.

Thermochemical Properties (Temperature 3450 K):

Property	H2O	LiBH4	TiH2/Al	C8H18/H2O2
* KJ of Elec En. (kJ/g)	10.0	14.33	1.058	1.0
Impetus (kJ/g)	1.6751	2.6802	0.8229	1.6945
Molecular Weight of the gas	17.633	10.535	2.33	16.841
Covolume (cm^3/g)	0.609	1.414	0.684	1.058
Gamma	1.2035	1.207	1.2728	1.2272
Eff. En. (kJ/g)	8.231	12.948	3.016	7.458
% Elec. En.	100%	100%	35%	13.4%
% Chem. En.	0%	0%	65%	86.6%
Density (g/cm^3)	1.0	0.868	2.16	1.26

*This term will be referred to as the electrical energy density.

III. CONDITIONS FOR OPTIMAL PERFORMANCE

As mentioned in the introduction, the pressure profiles within the gun are a function of the working fluid and electrical energy input. In theory, it is possible to tailor the electrical power input so as to precisely control chamber pressure for a given working fluid. Under this assumption, it is then possible to operate the system at a constant breech pressure, equal to the maximum allowable gun pressure. In theory, a constant breech pressure produces optimal projectile velocity if the energy source is confined to the combustion chamber as is the case considered in this study for the electrothermal gun.

The assumption that a constant breech pressure can be obtained imposes certain requirements on both the electrical energy input and working fluid. These requirements, however, are dependent on assumptions made concerning the interaction of the electrically generated plasma and working fluid. This interaction is complex and currently poorly understood. In fact, much of the initial experimental effort at BRL will be devoted to investigating plasma/working fluid interaction. In this paper two types of interaction will be investigated, uniform and non-uniform. For the initial set of calculations a uniform rate of interaction is employed. That is, it is assumed that, for a fixed amount of electrical energy input, a fixed amount of working fluid is transformed or dissociated into a gaseous mixture with fixed thermochemical properties. In this paper, dissociation refers to the conversion of the working fluid to its final state resulting from the interaction of the plasma with the working fluid. The thermochemical properties are those obtained from BLAKE for a specified amount of electrical energy per gram of working fluid. The values provided earlier in Table 2 are used for the initial set of calculations. No attempt is made in the simulations to model any effects due to the capillary and plasma creation. This process is considered as part of the overall electrical energy input.

Assumptions made for the ballistic simulations and comments are presented in Table 3.

TABLE 3: Assumptions For The Ballistic Simulations

1. The effects of the capillary are ignored. A complete transfer of electrical energy to the working fluid is assumed.
2. The gun geometry and projectile mass is given by Table 1.
3. The gun will operate at a constant breech pressure chosen to be 435 MPa to simulate ideal electrothermal performance.
4. Energy losses due to friction or shocked air in front of the projectile are not considered.
5. Energy losses due to heat transfer to the chamber and gun wall are ignored. At the present time the heat transfer mechanism for the electrothermal process is not well understood. It is hypothesized that the working fluid may reduce the amount of heat transfer. Experimental determination of heat transfer coefficients for various working fluids will be required before an adequate model for heat loss can be incorporated in the simulations.
6. A uniform rate of interaction between the working fluid and electrical energy input is assumed.
7. Gas temperature is not allowed to exceed 3450 K, which is felt to be an acceptable upper limit on propellant temperature.

In performing the initial calculations two lumped parameter interior ballistic computer codes are used. The first[7], written by the author, contained optimization routines to determine charge mass for constant breech pressure guns to obtain optimal velocity. Based upon the results of this code, IBHVG2[8], the second code, was used to obtain detailed ballistic profiles. In addition, IBHVG2 incorporates a gradient equation[9,10] which reflects the effects of having a chamber with chambrage. This gradient replaces the Pidduck-Kent or Lagrange gradient, both of which are known to be in error for high velocity or high charge-to-mass ratio simulations. Results using the chambrage gradient have been shown[11] to capture details in the pressure profiles and muzzle velocity which are nearer actual gun firing results and simulations using sophisticated hydrodynamic 1-D codes such as XNOVAKTC.[12] Results of the simulations for the different working fluids are summarized in Table 4. Breech and base pressure profiles are presented in Figures 2 through 5. It is noted that the velocities represent maximum values obtainable for the given gun and working fluid under the stated assumptions.

TABLE 4: Results Of Optimized Calculations

Property	H2O	LiBH4	TiH2/Al	C8H18/H2O2
Working Fluid Mass (g)	44.78	31.39	73.67	43.26
Muzzle Vel. (m/s)	2116	2339	1754	2128
Total Energy To Do Work (kJ)	368.6	406.4	222.2	322.6
Elec. Energy (kJ)	447.8	449.8	77.9	43.3
% Elec. En.	100%	100%	35%	13.4%
% Chem En.	0%	0%	65%	86.6%
Projectile KE (kJ)	40.3	49.2	27.7	40.8
Electrical Efficiency*	9%	10.9%	35.6%	94.2%
Ballistic Efficiency**	10.9%	12.1%	12.5%	12.6%
C/M***	2.49	1.74	4.09	2.40

* Ratio of projectile kinetic energy and electrical energy input.

** Ratio of projectile kinetic energy and the total energy to do work.

*** Ratio of working fluid mass and projectile mass.

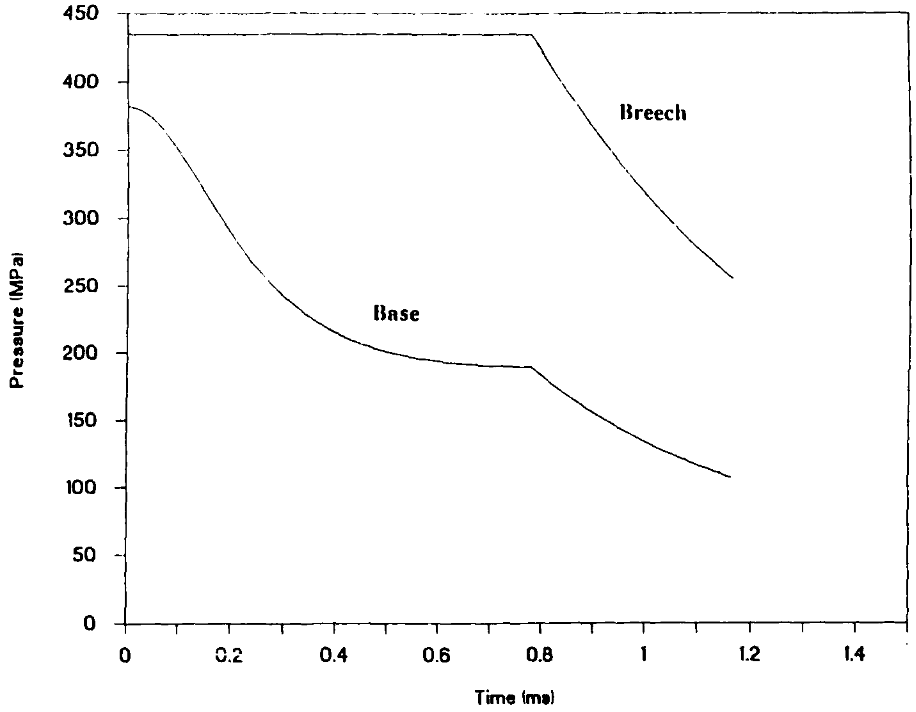

Figure 2: Breech And Base Pressure Versus Time For H2O

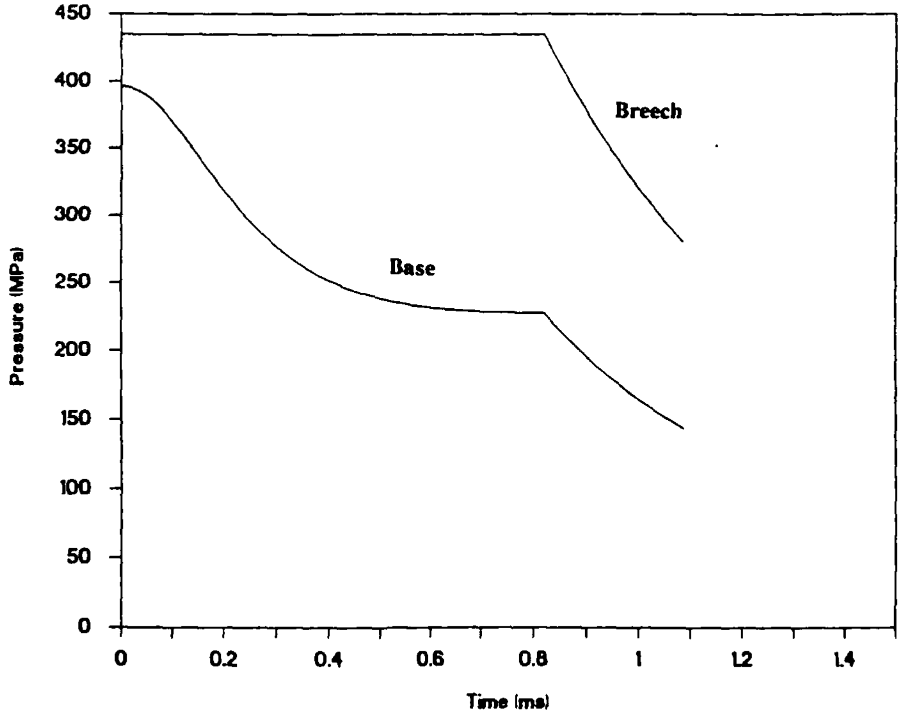

Figure 3: Breech And Base Pressures Versus Time For LiBH4

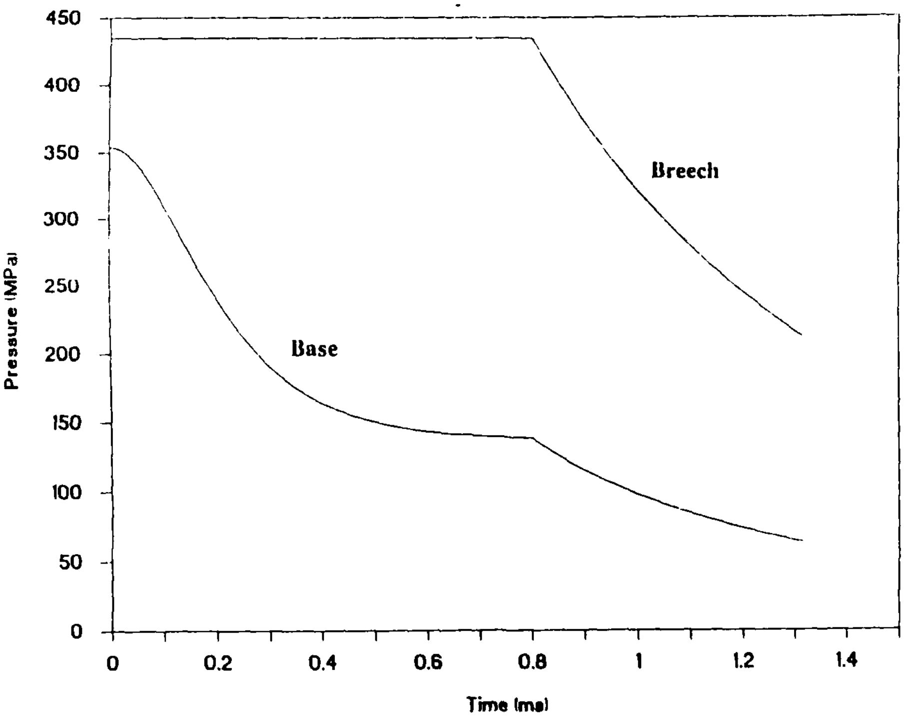

Figure 4: Breech And Base Pressures Versus Time For TiH2/Al

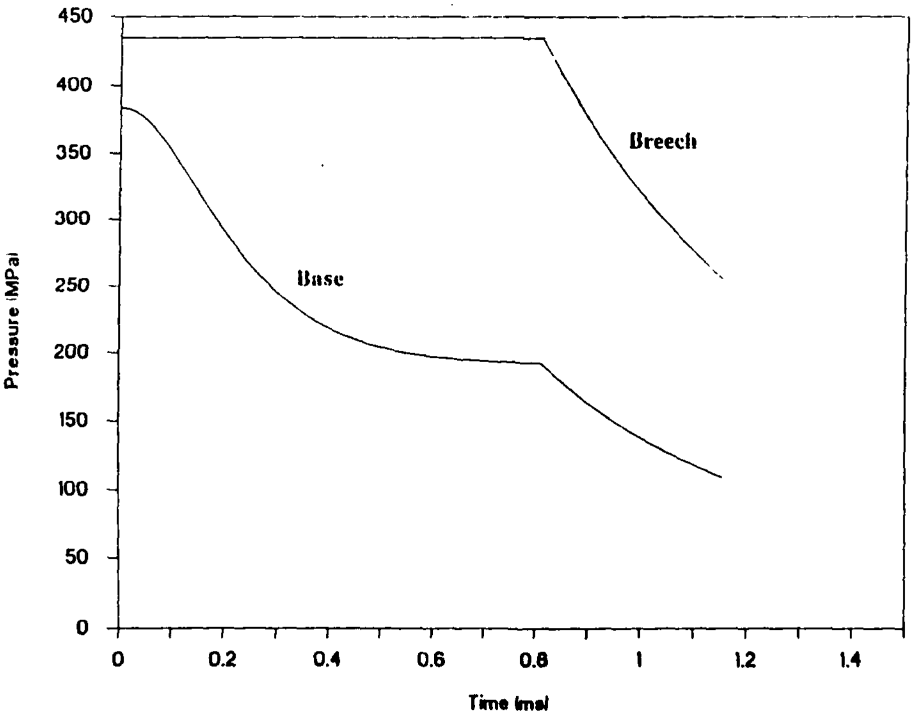

Figure 5: Breech And Base Pressures Versus Time For C8H18/H2O2

The results in terms of velocity, are what would be expected from a comparison of the impetus for each of the working fluids given in Table 2. The electrical and ballistic efficiencies are also consistent with ballistic expectations. Breech and base pressure/time profiles shown in Figures 2 through 5 are consistent with the thermochemical data with the exception of the TiH2/Al simulation. In Table 2, the molecular weight of the gas for this working fluid is 2.33. Such a low molecular weight gas should result in a small breech pressure to base pressure gradient (difference) due to the low mass of gas which needs to be accelerated.[13,14] Yet, it is evident from Figures 2 through 5 that the TiH2/Al mixture exhibits the largest pressure gradient or drop. However, the interaction of the plasma and the TiH2/Al mixture results in the formation of a large percent of solids, >90% Al_2O_3, TiO_2 and AlO_3,[15] which are either accelerated down the tube or represent energy sinks remaining in the chamber. In either case, the result is a reduction in energy and pressure. If both gas and solids are considered, the average molecular weight is closer to 32. Using this molecular weight brings the pressure gradient for the TiH2/Al working fluid into agreement with those shown in Figures 2, 3 and 5 for the other working fluids.

At this time it is not clear how to handle working fluids which produce a large percent of solids in the reaction with the plasma. Thermodynamically, using BLAKE, the solids are excluded from the impetus calculation. That is, the energy contained in the solids is not considered available to perform work. In addition, generally the equations used in interior ballistic calculations assume the propellant combusts to almost 100% gas which is the case for most solid propellants. However, it is hypothesized by some researches[19] in electrothermal propulsion that the solids do not remain in the chamber, but travel down the tube in thermal equilibrium with the gases. If this is the case, then a portion of the energy contained in the solids will be made available to perform work on the projectile resulting in improved performance over that predicted by the calculations given above. Although there is some experimental evidence[19] to support this claim, additional work, both experimental and theoretical, is needed in this area.

As indicated earlier, a major focus of this report is to investigate the conditions required of the electrical energy input and the working fluid to obtain the maximum velocity. Under the assumption of a uniform rate of interaction between the electrical energy input and working fluid, the power requirement can be obtained from the rate of mass change, an output of IBHVG2. Multiplying the electrical energy density (KJ/g) by the mass of working fluid consumed gives the electrical energy input, that is,

$$\text{Elec. Energy} = \text{Electrical Energy Density} * \text{Mass} \qquad (1)$$

or, letting EE stand for electrical energy, EERHO the electrical energy density and m the mass

$$EE = EERHO * m. \tag{2}$$

Now the assumption of a uniform rate of interaction between the electrical energy input and the working fluid implies EERHO is a constant. Therefore,

$$d(EE)/dt = EERHO * dm/dt. \tag{3}$$

However, electrical power is the time rate of change of electrical energy or d(EE)/dt. Thus, the electrical power is directly proportional to the mass rate of change. Applying this approach to the results of the optimal velocity calculations above produces the power versus time curves of Figure 6.

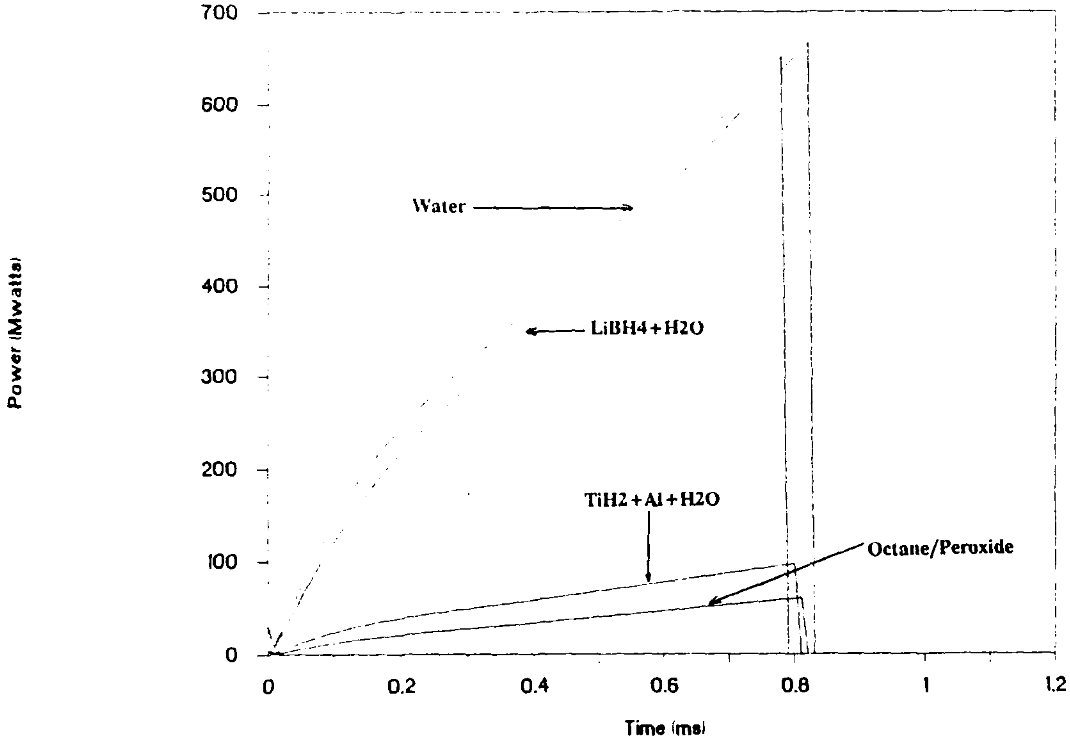

Figure 6: Power Versus Time Required To Produce Optimal Velocity For Various Working Fluids

The most striking feature of the curves is the distinction between the electrical energy requirements of the endothermic working fluids, H_2O and $LiBH_4$, and the exothermic fluids, TiH_2/Al and C_8H_{18}/H_2O_2. In all cases, the duration of the electrical pulse is about 0.8 ms, with no distinction apparent between the endothermic and exothermic fluids. The small drop at the beginning of the each curve is an artifact of the IB code. In the first computational time step the code calculates the amount of propellant that must be consumed in order to obtain the desired breech pressure. Thus, the first time step has an artificially high dm/dt which is corrected on the second time step resulting in a drop of dm/dt. The overall shape of the four curves, although more pronounced for the endothermic working fluids, is the same, an almost parabolic curve followed by a nearly linear portion of reduced slope ending in an abrupt drop. Although this shape is somewhat different from the perfectly linear curve which is normally indicated as required to maintain a constant breech pressure, there is no advantage of one curve over the other in terms of physical generation of the power curve.[16] Even though the abrupt drop at the end of the power curves is a result of computer simulation, this type of termination for the electrical input is desirable in actual firings. Continual electrical energy input beyond the consumption of all the working fluid can result in undesirable increases in gas temperature.

Once the assumption concerning a uniform rate of interaction between the electrical energy and fluid is made, most conditions on the working fluid are fixed. The only exception concerns the actual physical manner in which the volume of reacting working fluid is obtained. Requiring a constant breech pressure fixes the amount of working fluid which must be dissociated in a unit of time, but it does not specify how that volume of fluid is obtained. For example, a small surface area could regress a large distance or the regression rate could be quite small with a large reacting surface area to yield the same volume of working fluid. Unfortunately, a regression rate for working fluid dissociation or combustion is unknown. Intuitively, in seems that the amount of reacting surface area should give some measure of the degree of turbulence and breakup of the working fluid. In the computer simulations which were performed, a regression rate for the working fluid is chosen and the necessary surface area to support the constant breech pressure is computed. The regression rate selected was that of solid propellant JA2, which, using a standard pressure dependent law is

$$r = 0.15545 * P^{.908} \quad (4)$$

where r is in cm/(sec-MPa) and P is in MPa. For a pressure of 435 MPa the rate of regression would be 38.7 cm/s. In all four simulations the required surface area increases as a function of time. In fact, the shape of the surface area versus time curve is identical to the power curve. The typical method of analyzing surface area is to plot the ratio of the current surface area to initial surface area. However, since all the curves would be the same as the corresponding power curve, only the final ratio, which is also the highest, is given. These values are found in Table 5.

TABLE 5: Maximum Surface Area Ratios

H2O -- 26.24

LiBH4 -- 24.27

TiH2/Al -- 21.35

C8H18/H2O2 -- 23.09

For solid propellants the maximum surface area ratio is on the order of 2 to 3, with the maximum value occurring well before propellant burnout. Thus, the surface area ratios of Table 5 are about an order of magnitude larger than for solid propellants. Also, it appears that there is little difference due to the type working fluid. If the constant breech pressure condition is to be obtained in actual firings, it may be necessary for the mechanical interaction between the electrical energy input (plasma) and working fluid to break the working fluid into a large number of reacting particles/droplets to support surface area ratios of this magnitude. It is important to realize that the surface area ratios are increasing, and the interaction process must continually produce an ever increasing number of reacting particles/droplets. Such a continual disintegration of the working fluid may be indicative of the necessity of a turbulent interaction mechanism which may have a strong impact on reproducibility for electrothermal gun systems. In all probability, this mechanism is also highly dependent on the combustion chamber geometry which could further complicate analysis and reproducibility.

Of course, the surface area ratios shown in Table 5 are dependent on the regression rate of the working fluid. It is unlikely that the actual rate for the fluids is that of JA2, so the ratios in Table 5 may be in error by a large amount. It is also possible that the regression rate may not be solely dependent on pressure as indicated by equation (4), but dependent on other factors which admit a constant pressure but an increasing regression rate, substantially lowering the surface area requirements.

In summary, it appears that the requirements to produce a constant breech pressure are feasible, at least for the electrical input. However, based upon the surface area analysis, very reactive conditions between the plasma and working fluid could be required for both endothermic and exothermic working fluids to maintain the constant pressure. Ballistic results do seem to favor the use of the endothermic working fluid over the exothermic fluids, Table 4. This is due to the lower molecular weight (gas and solids) for the endothermic fluids. However, only a limited number of working fluids are considered in this study and there may be exothermic fluids which result in the same or higher velocities. In addition, the benefit of the higher velocity for the endothermic fluids may be offset by the order of magnitude, 450 kJ to 43 kJ, (see Table 4) increase in electrical energy required by the endothermic fluids compared to the exothermic fluids. An important observation from the ballistic results concerns the TiH2/Al simulation. The velocity for this mixture is 1754 m/s which is 17% lower than the velocity for H2O. The molecular weight of the gas for the TiH2/Al working fluid is 2.33 and 17.633 for H2O. Hence, creating a working fluid which produces gases with a low molecular weight is not a guarantee of superior performance as has been claimed by many proponents of electrothermal propulsion.[1] Not only must the working fluid produce gases with low molecular weight to reduce the pressure gradient and the mass of gas which must be accelerated, but the mass fraction of the working fluid which transitions to the gas state must be high. The gases for the TiH2/Al have a low molecular weight but only represent a small mass fraction, < 10%, of the total working fluid mass. There is simply an insufficient number of moles of gas to do the necessary work.

IV. PARAMETRIC INVESTIGATIONS

The purpose of the parametric investigations is to assess the sensitivity of the electrothermal process to several factors which are believed to affect performance. This should provide indications of expected reproducibility between firings of the experimental program as well as identify the critical factors for performance and experimental investigation. Two factors will be considered in this study. They are:

1. the amount of working fluid consumed.
2. the interaction rate between the electrical energy input and the working fluid.

In this study, each factor is varied separately, that is, all the conditions found for the optimal performance in the previous calculations will be held fixed while the one factor is varied.

1. AMOUNT OF CONSUMED WORKING FLUID

In previous calculations it has been assumed that the working fluid was totally dissociated by the electrical energy input during the time duration of the electrical energy pulse to the gun. The purpose of the first parametric study is to investigate degradation or improvement in performance if all the working fluid is not consumed. For each of the working fluids considered, simulations are performed with the amount of working fluid consumed reduced by 5, 10, 20 and 30% from the amount used in the calculations for optimal performance. The working fluid which is not used is treated as an inert mass taking up volume, and totally or partially accelerating down the gun tube. Specifically, it is assumed that either 100%, 50% or 0% of the unreacted working fluid will remain in the chamber. Unreacted working fluid will reduce chamber volume, and the fluid accelerated down the tube will be treated by increasing the mass of the projectile. Since all other conditions are held fixed, the electrical input will be that used for the constant pressure calculations. The assumption of a uniform interaction of electrical energy input and working fluid has a significant effect on the thermochemical values for the gases, especially temperatures. Table 6 gives the electrical energy density for each working fluid for each percentage drop in the amount of working fluid consumed. Appendix A provides the thermochemical properties for the working fluids as a function of electrical energy density. To perform the calculations an existing IB code[17], equivalent to IBHVG2 in terms of predictive capabilities, was modified so that electrical energy was an input to the code.[18] This modification was necessary since altering the amount of working fluid consumed may not result in a constant breech pressure calculation as used for the optimized performance calculations of section III.

TABLE 6: Electrical Energy Density (kJ/g) For Various Working Fluids When The Amount of Working Fluid Consumed Is Decreased.

% Decrease	H2O	LiBH4	TiH2/Al	C8H18/H2O2
5%	10.53	15.08	1.11	1.05
10%	11.11	15.92	1.17	1.11
20%	12.50	17.91	1.32	1.25
30%	14.29	20.47	1.51	1.43

Of special interest is the increase in gas temperature which occurs when the amount of working fluid consumed decreases. Figure 7 summarizes the percent increase in the computed thermochemical flame temperature of the gases for the different working fluids and decreases in amount of working fluid consumed. The original temperature of each working fluid/electrical energy combination was approximately 3450 K. The maximum temperatures obtained with the 30% reduction in working fluid consumed are given in Table 7.

TABLE 7: Maximum Theoretical Gas Temperatures For A 30% Reduction In Working Fluid Consumed

H2O -- 4416 K
LiBH4 -- 3954 K
TiH2/Al -- 3592 K
C8H18/H2O2 -- 3600 K

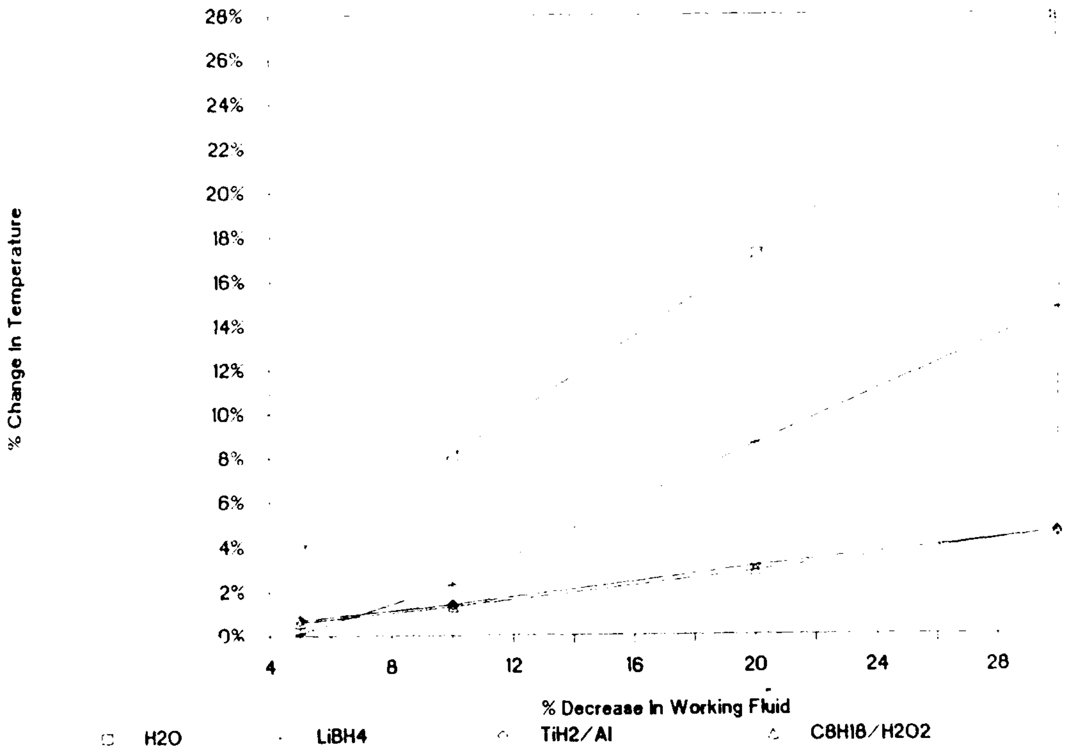

Figure 7: Percent Change in Temperatures For Decreased Working Fluid Consumed - Reference Temperature 3450 K

As can be seen from Figure 7 the percent increase in temperature appears to be heavily dependent on whether the fluid is endothermic or exothermic. Even for large decreases in the mass of working fluid consumed, the flame temperature rose only a modest 3% to 4% for the exothermic fluids. On the other hand, H2O exhibits an almost 1-1 correspondence between the percent increase in temperature and percent decrease in mass of working fluid. The LiBH4 falls between the two extremes except for the 5% loss in working fluid. These trends are not unexpected, since the endothermic fluids obtain all their energy from the electrical energy source, whereas the electrical energy requirements for the exothermic fluids are much lower (see Table 2). Thus, when the amount of working fluid is reduced, the total energy supplied to an endothermic fluid remains the same, but the total energy for the exothermic fluid is decreased by the amount of chemical energy stored in the deleted working fluid. Now, with the reduced amount of working fluid, the electrical energy can be thought of as being divided into two portions, that amount which will take the remaining working fluid to the original state, ~3450 K, and the excess which would have been used to bring the removed working fluid to the same temperature. This excess electrical energy, which is significantly larger for the endothermic fluids, produces the increase in temperature. Thus, the temperature increase would be larger for the endothermic fluids. The magnitude of the increase is dependent not only on the excess energy available, but also on the complexity of the gas molecules since the more complex molecules have higher heat capacities which require more energy to raise the gas temperature. This may explain the difference in the magnitude of the temperature increase between the H2O and LiBH4. However, the lower temperature of the LiBH4 at the 5% reduction in working fluid appears inconsistent and should be investigated in more depth with a detailed analysis of constitutive products of the different fluids at that temperature. Not surprisingly, the sensitivity of temperature change to decrease in working fluid mass, measured by the slope of the curves, is greater for the endothermic fluids.

Results of the simulations are presented in Figures 8 through 10 for velocity changes and in Figures 11 through 13 for changes in maximum chamber pressure.

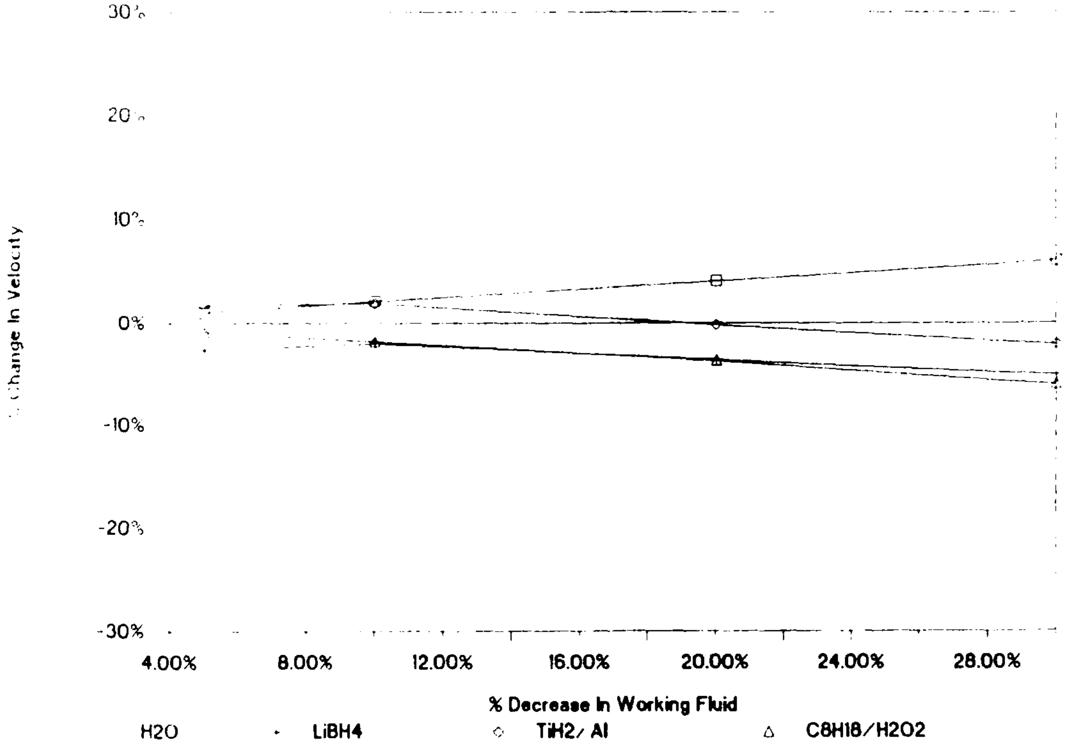

Figure 8: Velocity Changes-100% of Excess Working Fluid in Chamber

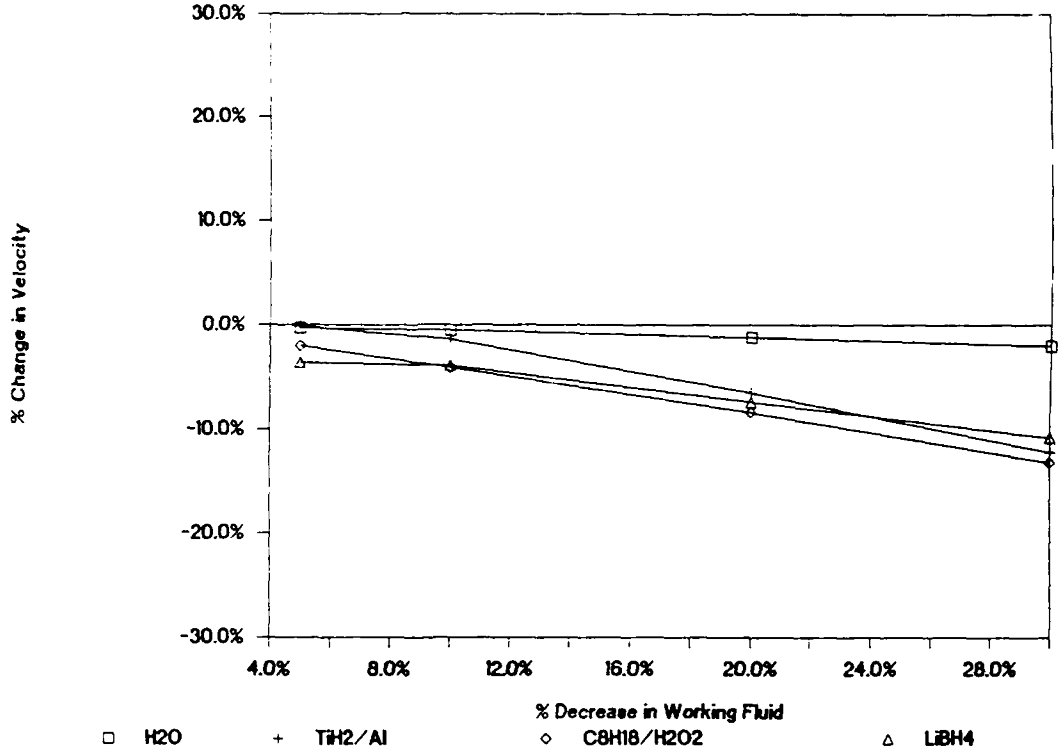

Figure 9: Velocity Changes-50% of Excess Working Fluid in Chamber

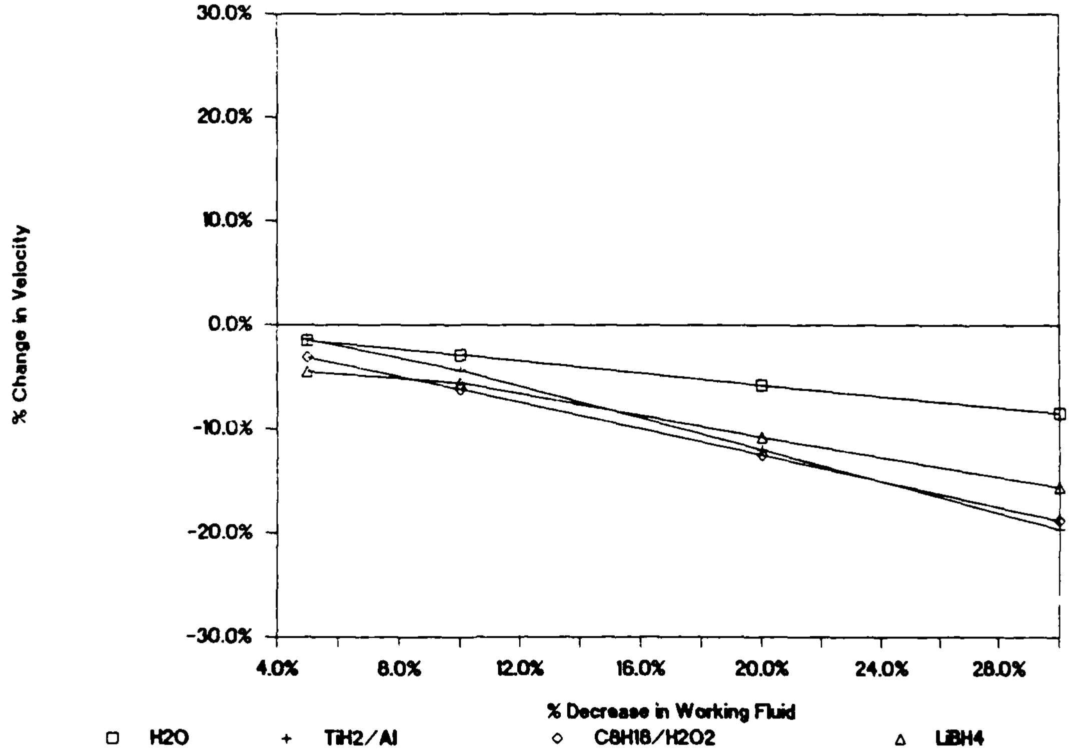

Figure 10: Velocity Changes-0% of Excess Working Fluid in Chamber

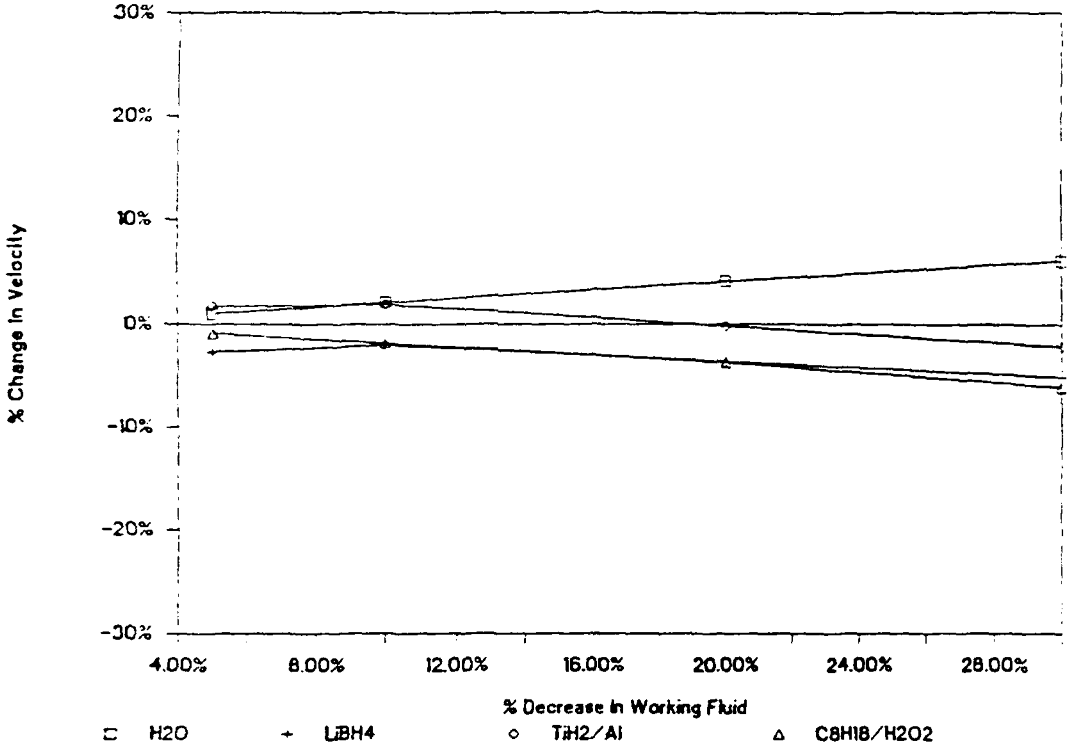

Figure 11: Pressure Changes-100% of Excess Working Fluid in Chamber

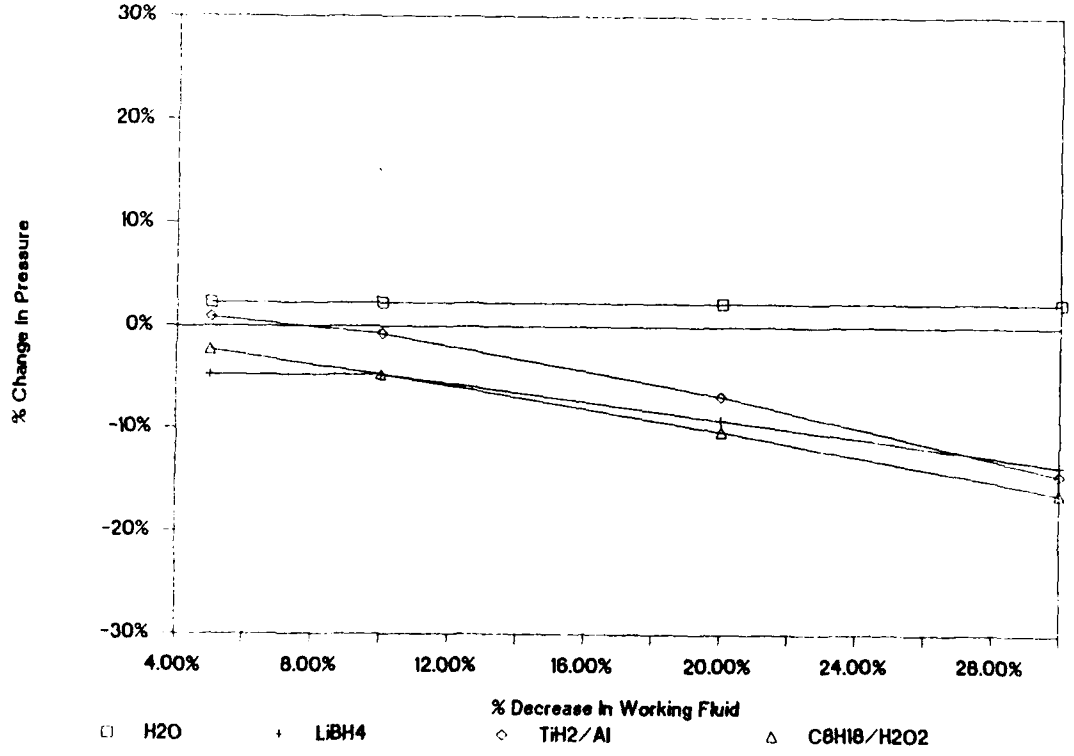

Figure 12: Pressure Changes-50% of Excess Working Fluid in Chamber

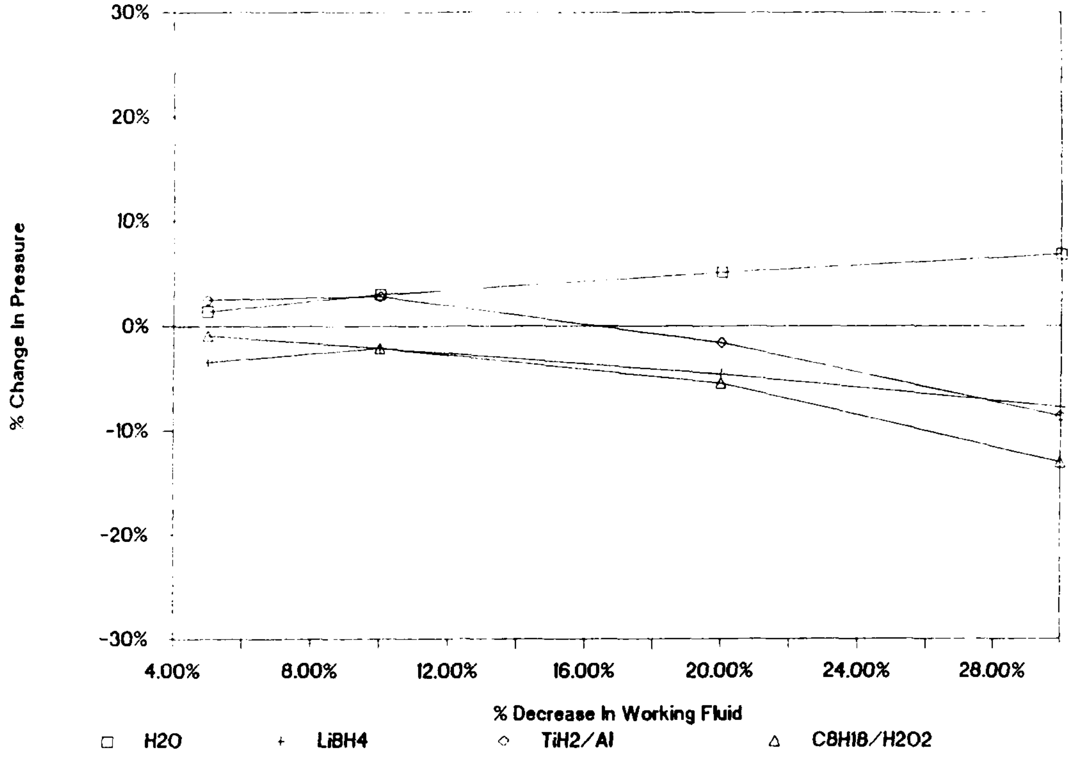

Figure 13: Pressure Changes-0% of Excess Working Fluid in Chamber

To summarize velocity results, two trends should be expected. First, as the amount of working fluid consumed decreases the total available energy for endothermic fluids will remain the same since all energy is due to the external electrical energy source. On the other hand, for the exothermic fluids the amount of available energy will drop by about the same percentage as the decrease in working fluid mass. Thus, velocity for endothermic fluids should remain about the same as in the constant pressure calculations of section III. On the other hand, the velocity would be expected to drop for the exothermic fluids. The second trend which would be expected is that velocity will decrease as the amount of unreacted working fluid which is accelerated down the tube increases since accelerating the unreacted working fluid will require an additional amount of energy. These trends are clearly evident in Figures 8 through 10 except for the LiBH4 working fluid which exhibits velocity decreases more in line with the exothermic fluids than the endothermic H2O. One reason for this behavior is that as the electrical energy density increases for the LiBH4 the percent of the electrical energy which is available to perform work decreases, unlike H2O where the percent of usable energy remains constant. This is illustrated in Table 8. Thus, using LiBH4 is similar to using an exothermic working fluid, that is, as the amount of working fluid consumed decreases the available energy decreases.

TABLE 8: Percent Of Available Energy For H2O and LiBH4 For Various Electrical Energy Densities

	Electrical Energy Density (kJ/g)	Percent of Available Energy
H2O:		
	10	82.3%
	11	82.5%
	12	82.2%
	13	81.5%
LiBH4:		
	14	88.6%
	15	86.8%
	16	85.3%
	17	84.2%

As for maximum chamber pressures shown in Figures 11 through 13, there is no intuitive expected result. Less energy for the LIBH4 and the exothermic fluids should result in lower pressures. However, this could be offset by the slower increase in volume resulting from reduced projectile velocity due to the lower energy and/or the heavier effective projectile mass when the unreacted fluid is accelerated down the tube. Also, having unreacted working fluid reduces chamber volume and hence could result in higher chamber pressures. For the H2O, since the energy remains constant, pressures should increase for the case of unreacted working fluid accelerating down tube due to the lower rate of volume increase. When all unreacted working fluid remains in the chamber, the decreased chamber volume appears to be offset by increased volume expansion since the projectile velocity is higher for H2O in this case (see Figure 8). From Figures 11 through 13, it appears that, in general, the reduced energy has a greater effect on the pressures than the decreased chamber volume and lower volume increase for LiBH4 and exothermic working fluids. Thus, lower chamber pressures are observed in all cases except for TiH2/Al when the amount of unreacted working fluid is small and totally or partially accelerates down the tube, see Figures 12 and 13. H2O shows the expected increases in pressure when unreacted working fluid is accelerated down tube, Figures 12 and 13. But the increased velocity and, thus, increased volume expansion appears to more than compensate for the reduced chamber volume when all the unreacted working fluid remains in the chamber and a lower maximum chamber pressure is predicted (Figure 11). Although an increase in velocity is predicted with a lower maximum chamber pressure, Figures 8 and 11, using H2O it should be remembered that this was obtained only at the expense of significantly higher gas temperatures, up to ~4400 K.

2. INTERACTION RATE

In the second parametric study the interaction rate between the electrical energy input or plasma and working fluid is varied. Under ideal working operation, an electrothermal gun would exhibit a uniform rate of interaction between the plasma and working fluid. This means that the total mass of working fluid is completely dissociated at the exact instant the electrical input ceased and that the amount of working fluid dissociated for every unit of electrical energy input is the same. These conditions are equivalent to assuming that the working fluid acts in the same manner as a solid propellant, with the electrical input determining the burn rate. In the context of a rate of interaction, a uniform rate can be thought of as meaning that the percent of working fluid dissociated at any time is always equal to the percent of the total electrical energy which has been transmitted to the system. Graphically this is shown in Figure 14 by the curve labeled Uniform. However, in practice there may be variations in the interaction rate.

For the study, three alternate interaction rates are investigated and are presented graphically in Figure 14. For the first, labeled 2*, the working fluid is dissociated in such a way that the percent dissociated is twice the percent of electrical energy input. Thus, the working fluid will be totally dissociated at 50% electrical input. In the second, labeled .5*, the working fluid dissociates at half the rate. Once the total electrical input has been completed the remaining 50% of the working fluid will dissociate at a rate which has complete dissociation just before projectile exit. The final rate, labeled Sine, has a slower rate for the first 50% of electrical energy input and a higher rate thereafter until completion of the electrical input at which time the working fluid has been totally dissociated. Specifically, the Sine curve was obtained by fitting a 4th degree polynomial to the points (0,0), (25,15), (50,50), (75,90) and (100,100). The purpose in selecting these interaction rates was to bracket the extremes, 2* and .5*, and to investigate small perturbations about the uniform rate, Sine.

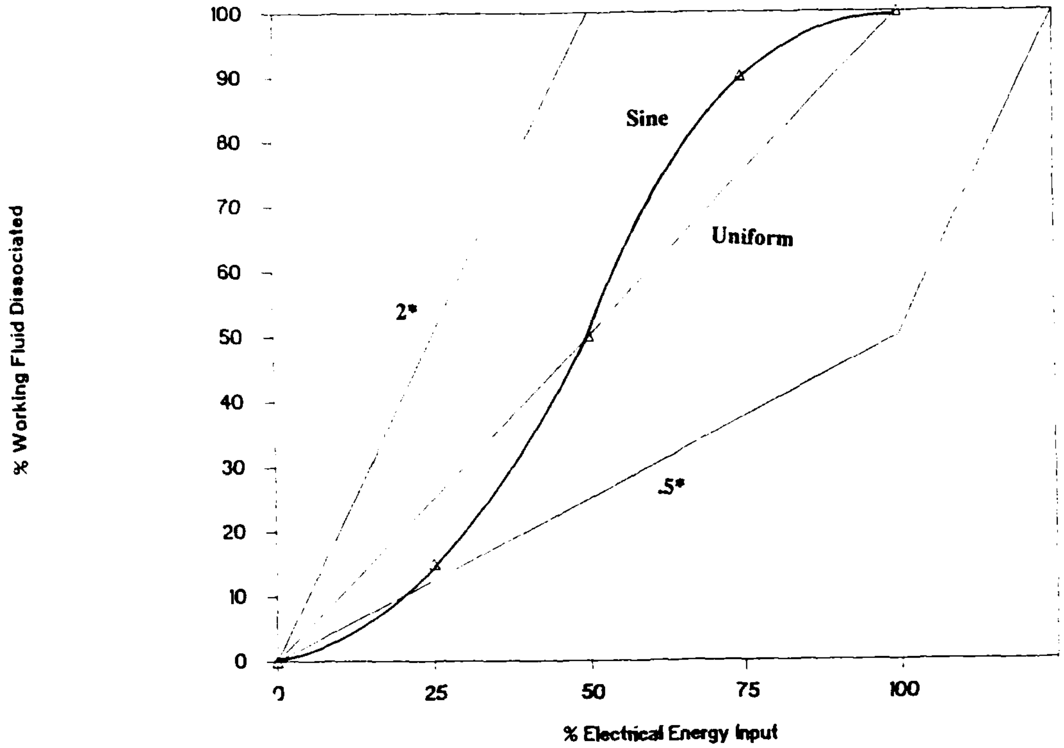

Figure 14: Interaction Rates Utilized In The Study

As a consequence of changing the rate of interaction, the electrical energy density and, hence, thermochemical properties will no longer be constant during the ballistic event as is assumed for solid propellant IB calculations. To account for changing thermochemical properties, the IB code used in the previous parametric study was further modified to determine the appropriate thermochemical values for the electrical energy density on each time step. As for other assumptions, since the quantity varied is the interaction rate, the power curve and working fluid charge mass were those determined by the earlier constant pressure calculations of section III. Thus, for a given working fluid, the total energy in each simulation is the same as the constant pressure calculation. Finally, simulations were performed for one endothermic, H2O, and one exothermic, C8H18/H2O2, working fluid.

As before, the quantities of interest are projectile muzzle velocity, pressures and temperature. Velocity results together with the results for the uniform, constant pressure, calculations are presented in Table 9.

TABLE 9: Ballistic Results Using Various Interaction Rates With H_2O and C_8H_{18}/H_2O_2

Working Fluid: H_2O

Option	Velocity (m/s)	% Difference with Uniform	Pmax (MPa)
2*	1873	-11.5%	367
.5*	2196	+3.8%	472
Sine	2161	+2.1%	527
Uniform	2116	0.0%	435

Working Fluid: C_8H_{18}/H_2O_2

Option	Velocity (m/s)	% Difference with Uniform	Pmax (MPa)
2*	2408	+13.2%	816
.5*	1877	-11.8%	379
Sine	2224	+4.5%	579
Uniform	2128	0.0%	435

As indicated by Table 9, H_2O appears to be less sensitive than C_8H_{18}/H_2O_2 to the change in interaction rate. As would be expected, both show the smallest percent change for the Sine option which was the moderate perturbation. For the extreme cases, 2* & .5*, however, results are quite different. The velocity for H_2O decreases for the 2* option and moderately increases for the .5* option. Just the opposite is true for the C_8H_{18}/H_2O_2 working fluid, showing a large increase for the 2* option and a large decrease for the .5* option. The behavior for the extreme cases can be understood by investigating the breech pressure profiles shown in Figures 15 and 16 and computed gas temperatures shown in Figures 17 and 18. However, before presenting the analysis it is important to note that the area under the pressure curves appears to correspond to the muzzle velocities shown in Table 9. In fact, the pressures indicate a much greater sensitivity for C_8H_{18}/H_2O_2, almost 450 MPa difference in pressure, than is indicated from a comparison of velocities only.

First an analysis for the 2* option is presented. Intuitively it would seem that the 2* option should result in larger pressures earlier in the ballistic cycle, since more material is being consumed. Option 2* is analogous to doubling the burning rate for solid propellants. However, unlike solid propellants, the electrical input represents an additional energy source and is the same in all simulations for a given working fluid. It is the combination of these two factors, mass consumed and the amount of electrical energy input at the current time step which determine the resulting pressure. In this report electrical energy density, defined by mass consumed/ electrical energy input, has been the measure of the relative relationship of these two quantities. Now consider option 2* with H2O. Until half way through the input of the electrical energy the same amount of energy as in the uniform case but twice the amount of H2O will be reacted in the system. Thus, twice the amount of energy, since there is twice as much fluid, will be used to simply dissociate the working fluid to the gaseous state. In addition, the remaining energy, used to heat the gases and create pressure, is diluted by having to operate on a larger mass of gas. This is reflected in the lower pressure shown in Figure 15 and lower temperature of Figure 17. Finally, the lower pressure translates into reduced force on the projectile and lowered velocity. For the exothermic fluid, C8H18/H2O2, however, having twice the mass means having almost twice the available energy, since about 90% of the usable energy is stored in the working fluid. Thus, the higher pressure of Figure 16 and increased velocity would be expected.

A similar type argument holds for the .5* option. For H2O, there will be half as much fluid, but the same amount of energy. This should provide more energy to heat the gas, as shown in Figure 17, and increase pressure, Figure 15. One factor which will tend to lower the pressure is that there will be half the number of moles of gas. These conflicting factors, at least for pressure, explain why even for the hotter gas the pressure for the .5* option is only about that of the uniform calculation, 435MPa. Using C8H18/H2O2 with the .5* option will substantially lower the amount of energy which will tend to lower pressure as shown in Figure 16. Analysis of the Sine option requires a combination of both of the preceding arguments since this option has features of both the 2* and .5* options. The pressure, Figures 15 and 16, and temperatures, Figures 17 and 18, are consistent with such arguments and will not be presented.

As discussed in the previous paragraphs, the flame temperatures in Figures 17 and 18 are consistent with the different assumptions of the interaction rates. However, the large difference in temperature fluctuation exhibited by the endothermic fluid, 1900 K to 5500 K, in comparison to the exothermic fluid, 3200 K to 3750 K, highlights a disadvantage associated with using endothermic working fluids. When the electrical source supplies a large percentage of the total energy, as for the endothermic case, if a sufficient amount of working fluid is not being dissociated the excess electrical energy will result in substantial increases in gas temperature.

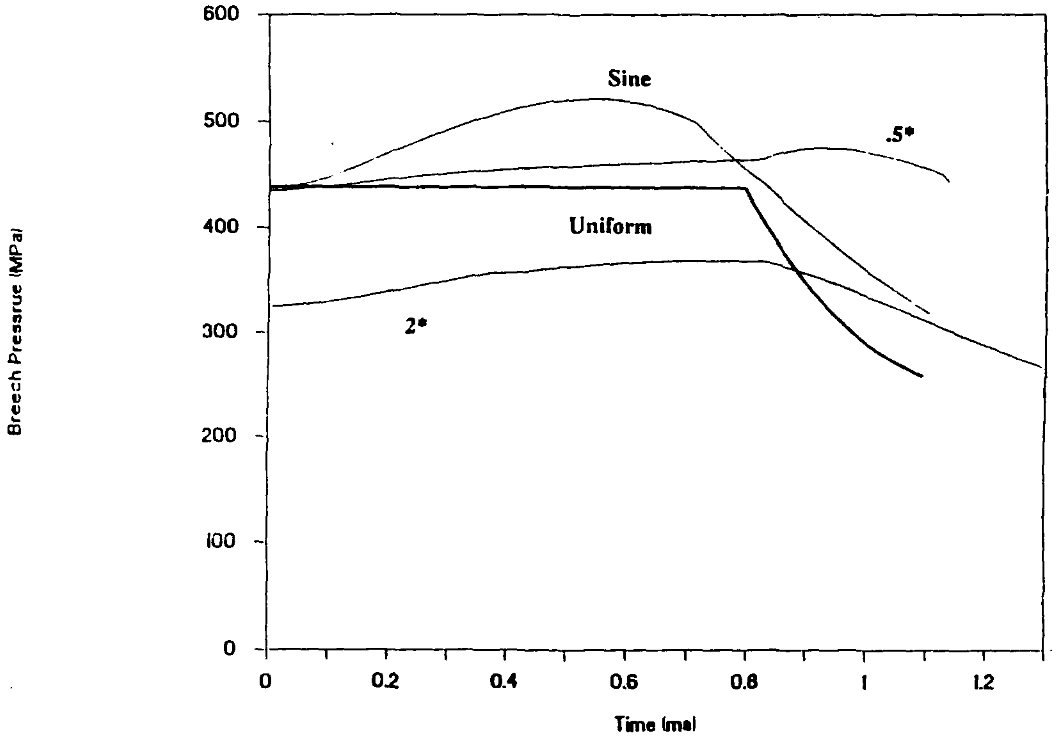

Figure 15: Breech Pressure For Various Interaction Rates -- H2O

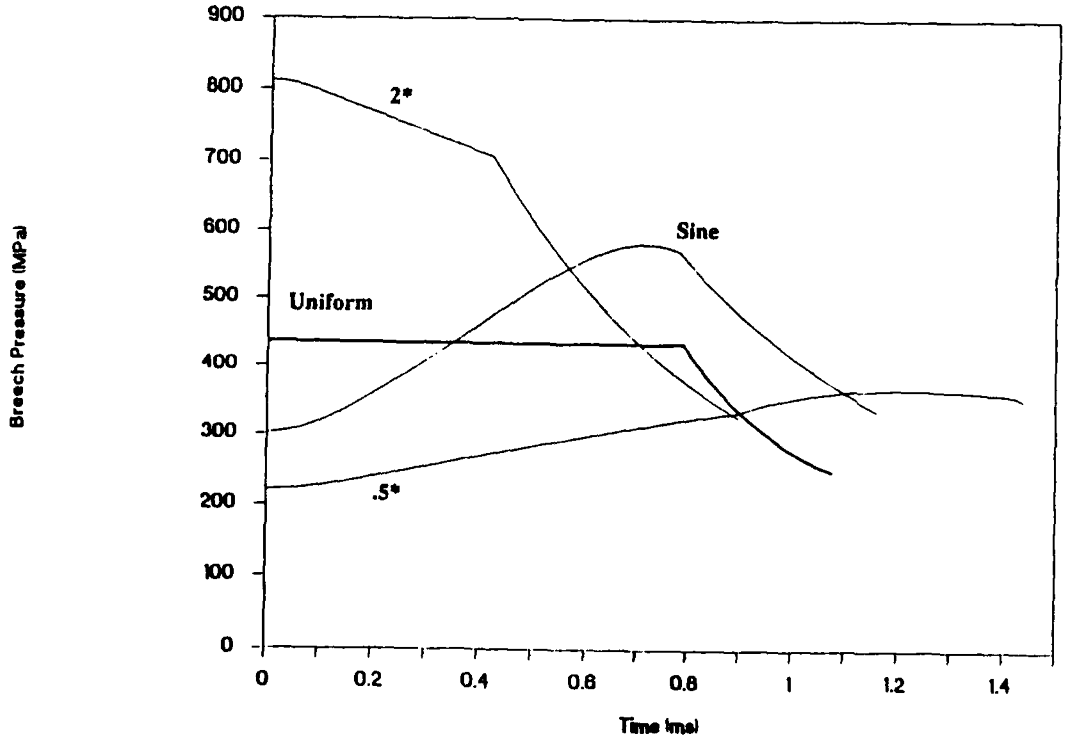

Figure 16: Breech Pressure For Various Interaction Rates -- C8H18/H2O2

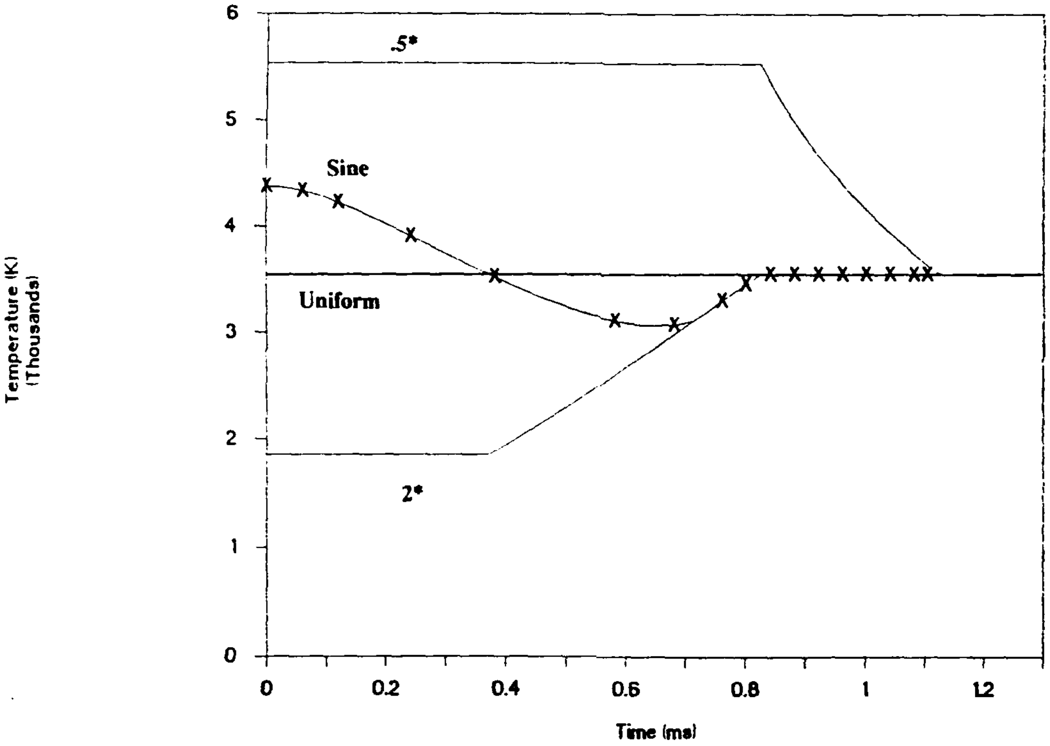

Figure 17: BLAKE Flame Temperature For Various Interaction Rates -- H_2O

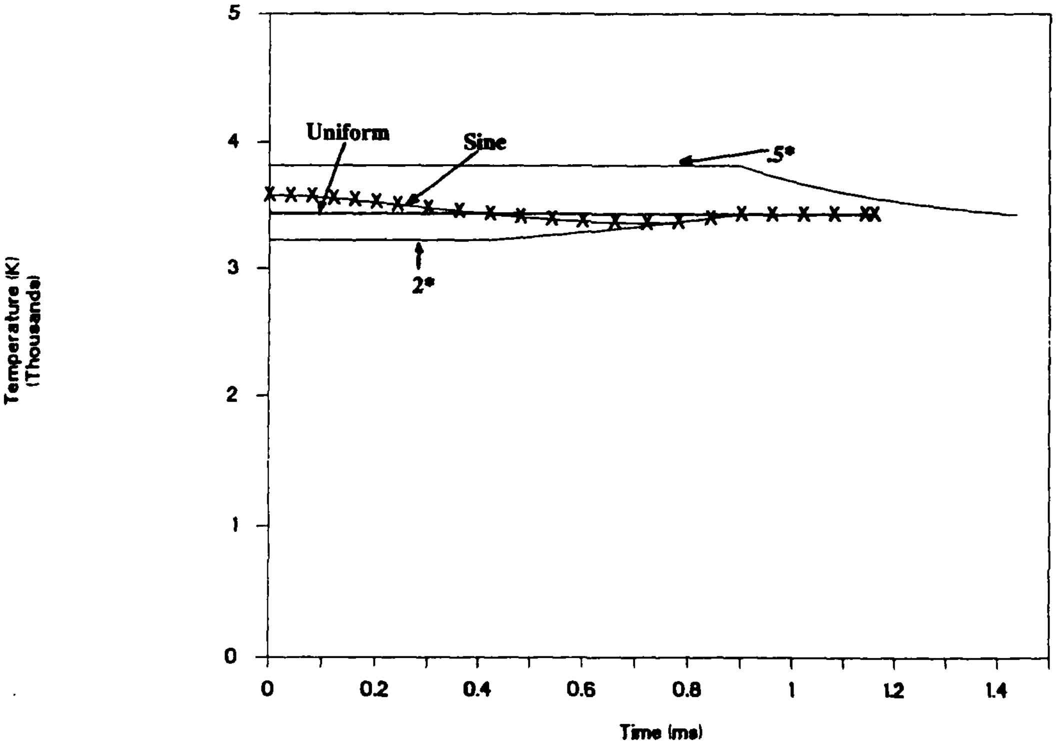

Figure 18: BLAKE Flame Temperature For Various Interaction Rates -- C_8H_{18}/H_2O_2

To summarize, it appears that there are significant differences between endothermic and exothermic working fluids if the interaction rate between electrical energy and working fluid varies. Exothermic fluids exhibit greater variability in terms of pressure and velocity. Yet, computed fluctuations in gas temperature are small. On the other hand, the endothermic working fluid does not show as large a variation in pressure and velocity measurements, but produces large changes in gas temperature. This is especially worrisome if the amount of working fluid actually reacting with the plasma is less than expected. In the case studied, option .5*, pressure, Figure 15, and velocity, Table 9, are almost identical to the constant pressure calculations, but the gas temperature, Figure 17, is 2000 K higher!

V. COMPARISONS

It is important to ascertain the potential benefits of any proposed technology relative to that in current use. Toward that end, comparisons in terms of velocity are made between electrothermal and solid propellant simulations. For the solid propellant calculations a JA2 propellant is assumed. The electrothermal simulations were performed using the four working fluids discussed in this report with the amount of electrical energy input adjusted to provide gas temperatures equivalent to JA2, that is, the same conditions as used in the optimal velocity calculations performed in section III. The gun envelope is that used earlier as given in Table 1. Calculations for the solid propellant cases were performed using IBHVG2 and XNOVAKTC. Two solid propellant simulations were performed. The first involved varying grain geometry and mass to obtain the highest velocity under a breech pressure constraint of 435 MPa. This series of calculations gives the highest velocity which in practice can currently be obtained with solid propellants and is considered for purposes of computing percent differences with the other simulations as the baseline case. The second simulation was a constant breech pressure calculation imposing the 435 MPa constraint. This calculation provides the highest velocity which can be obtained using ideal solid propellant. In addition, since the constant breech pressure assumption is the same as that used in the ET simulations, this calculation also indicates if there is any inherent advantage of using a working fluid in place of a solid propellant. For the ET simulations the constant breech pressure calculations of section III are used. In all simulations no heat loss was considered. Results are summarized in Table 10.

TABLE 10: Comparison Of ET And Conventional Simulations

Type Simulation	Propellant/ Working Fluid	Charge Mass (g)	Velocity (m/s)	%Diff. with Conv.	Elec. Energy (KJ)
Conventional Geometry Varied	JA2	58 (1-perf)	1891	NA	0.0
Conventional Constant Breech	JA2	56.36	1945	+ 2.9%	0.0
ET	H2O	44.78	2116	+11.9%	448
ET	LiBH4	31.39	2339	+23.7%	450
ET	TiH2/Al	73.67	1754	- 7.2%	78
ET	C8H18/H2O2	43.26	2128	+12.5%	43

A comparison of the velocities shows that electrothermal guns can substantially out perform conventional solid propellant systems, by as much as a 23.7% increase, given the correct choice for the working fluid in the system being studied. However, as Table 10 indicates, a large amount of electrical energy is required to realize this advantage. The moderate increases for H2O and C8H18/H2O2 indicate that one of the basic underlying assumptions for the electrothermal process may be valid, in that greater velocity can be achieved using the lighter molecular weight gases. This point is further underscored by comparisons with the constant breech pressure conventional calculation where the only difference with the ET simulation is the molecular weights of the gases. However, the low velocity figure for the TiH2/Al illustrates that care must be taken in pursuit of lighter molecular weight gases. The percentage of solids which are formed from the interaction of the plasma and working fluid must not be large. Solid particles are energy sinks and reduce the effective energy of the mixture. An analogous way to view the situation is that a high percentage of solids reduces the mass or number of moles of gas, n, which when applied to the equation of state

$$P * V = n * R * T \qquad (5)$$

would result in lower pressure, P, for fixed volume, V, and temperature, T, with R the universal gas constant. Lower pressures, of course, result in lower velocity. This is not a problem for solid propellant, since almost all of the propellant transitions to a gaseous state, but it can be for certain working fluids in the electrothermal process. In analyzing the electrothermal process it is important to remember that some of the equations of interior ballistics have assumed that the propellant transitions almost entirely to a gas, and, thus, the assumption must be corrected if a significant amount of the dissociated working fluid is solids.

To summarize, the comparisons indicate that ET propulsion can out perform convention solid propellant systems with no penalty in gas temperature, at least for the system under study. However, the magnitude of the increase is very dependent on the choice of working fluid. In fact, a poor choice of working fluid can result in decreased performance.

VI. CONCLUSIONS

This work is not intended to be an exhaustive study of the operating characteristics of the electrothermal process. This goal can not be realized without the development of a sophisticated, hydrodynamic code which accurately models the complex interaction processes between plasma and working fluid and which has also been validated by experimental results. The purpose of this report is to investigate conditions for favorable ET performance as well as conditions which can result in a degradation of this performance and ballistic variability. Results can be summarized as follows.

> Conditions to achieve optimal performance utilizing the constant breech pressure gun have be investigated. Although the electrical power input appears feasible, obtaining the proper fluid vaporization/combustion rate may be difficult and could be a source of variability in experimental firings.
>
> The ET concept can out perform conventional solid propellants at comparable gas temperatures, at least for the gun envelope studied. However, the choice of working fluid is critical.
>
> For the electrothermal process, pressure, velocity and temperature variability is strongly dependent on the plasma-working fluid interaction process. This has important implications for experimental programs. Seemingly identical firings may produce vastly different results due to changes in the interaction process caused by any one of a number of factors.
>
> Endothermic working fluids show less pressure and velocity variability than exothermic working fluids. However, this greater stability in pressure and velocity is offset by large fluctuations in gas temperature.

REFERENCES

1. Juhasz, A.A., Jamison, K., Wren, G.P. and White, K.J., "Introduction to Electrothermal Gun Propulsion," 25th JANNAF Combustion Meeting, NASA Marshall Space Flight Center, Huntsville, AL., October 1988.

2. Oberle, W.F. , Wren, G.P., Robbins, F.W., White, K.J.,Tompkins, R.E. and Juhasz, A.A., "Parameters For Optimizing A Traveling Charge Gun System," BRL Technical Report BRL-TR- 2910, Ballistic Research Laboratory, Aberdeen Proving Ground, MD., May 1988.

3. Greig, J.R., "Electrothermal Gun Program Status Report," Ballistic Research Laboratory, Aberdeen Proving Ground, MD., May 1988.

4. Gora, T., "Proceedings of the Workshop on Electrothermal Accelerators," Picatinny Arsenal, N.J., October 1987.

5. Freedman, E., "BLAKE - A Thermodynamics Code Based on TIGER:
User' Guide and Manual," BRL Technical Report ARBRL-TR-02411, Ballistic Research Laboratory, Aberdeen Proving Ground, MD., July 1982.

6. Bunte, S.W. and Oberle, W.F., "An Analysis of the Thermochemical Performance of Various Working Fluids for an Electrothermal Gun," 25th JANNAF Combustion Meeting, NASA Marshall Space Flight Center, Huntsville, AL., October 1988.

7. Oberle, W.F., Unpublished work, Ballistic Research Laboratory, Aberdeen Proving Ground, MD., 1988.

8. Anderson, R.D. and Fickie, K.D., " IBHVG2 -- A User's Guide," BRL Technical Report BRL-TR-2829, Ballistic Research Laboratory, Aberdeen Proving Ground, MD., July 1987.

9. Wren, G.P. and Morrison, W.F., "Velocity and Pressure Distributions in the Liquid Reservoir in a Regenerative Liquid Propellant Gun," BRL Technical Report BRL-TR-2933, Ballistic Research Laboratory, Aberdeen Proving Ground, MD., September 1988.

10. Robbins, F.W., Anderson, R.D. and Gough, P.S., "Continued Studies of the Development of a Modified Pressure Gradient Equation for Lumped-Parameter Interior Ballistic Codes," work in progress, Ballistic Research Laboratory, Aberdeen Proving Ground, MD., 1988.

11. Robbins, F.W. and Keller, G.E., "Studies Supporting Development of a Modified Gradient Equation for Lumped- Parameter Interior Ballistic Codes," BRL Memorandum Report BRL-MR-3678, Ballistic Research Laboratory, Aberdeen Proving Ground, MD., July 1988.

12. Gough, P.S., "The NOVA Code: A User's Manual. Volume 1. Description and Use," IHCR 80-8, Naval Ordnance Station, Indian Head, MD, December 1980.

13. Corner, J., "Theory of the Interior Ballistics of Guns," John Wiley & Sons, Inc., New York, New York, 1950.

14. Hunt, F.R.W., ed., "Interior Ballistics," The Philosophical Library, Inc., New York, New York, 1951.

15. White, K.J. and Tompkins, R.E., Private Communications, Ballistic Research Laboratory, Aberdeen Proving Ground, MD., 1988.

16. Zielinski, A., Private Communications, Ballistic Research Laboratory, Aberdeen Proving Ground, MD., 1988.

17. Robbins, F.W. and Raab, T.S., "A Lumped-Parameter Interior Ballistic Computer Code Using the TTCP Model," BRL Memorandum Report BRL-MR-3710, Ballistic Research Laboratory, Aberdeen Proving Ground, MD., November 1988.

18. Oberle, W.F., Unpublished work, Ballistic Research Laboratory, Aberdeen Proving Ground, MD., 1988.

19. Goldstein, S. A., Private Communications, GT Devices, Alexandira, VA, February, 1989.

APPENDIX A

Thermochemical Values for Various Working Fluids in Combination with Electrical Energy Input

TABLE A-1. Water

Working Fluid: Water (H_2O)

Electrical Energy Input	Temperature	Pressure	Impetus	Molecular Weight	Covolume	Gamma	Effective Energy
kJ/g	K	MPa	J/g	(-)	cm^3/g	(-)	kJ/g
3	917	61.92	423.1	18.015	-1.834	1.9414	0.44
4	1413	122.13	652.3	18.014	-0.342	1.4	1.63
5	1855	174.11	856.4	18.014	0.082	1.2987	2.86
6	2261	221.38	1044.2	18.001	0.283	1.2557	4.08
7	2633	265.08	1218.3	17.967	0.404	1.2323	5.24
8	2971	305.89	1380.1	17.896	0.488	1.2182	6.32
9	3276	344.47	1531.6	17.783	0.554	1.2093	7.31
10	3552	381.53	1675.1	17.633	0.609	1.2035	8.23
11	3805	417.67	1813.1	17.45	0.659	1.1998	9.07
12	4038	453.37	1947.3	17.242	0.705	1.1975	9.85
13	4256	489.03	2079.6	17.015	0.748	1.1962	10.59
14	4461	524.88	2210.9	16.775	0.788	1.1958	11.29
15	4655	561.15	2342.2	16.526	0.826	1.1959	11.95
16	4842	597.99	2474	16.272	0.863	1.1964	12.59
17	5022	635.56	2607.2	16.015	0.898	1.1973	13.21
18	5196	673.92	2741.9	15.757	0.931	1.1985	13.81
19	5366	713.12	2878.3	15.501	0.964	1.1998	14.40
20	5533	753.27	3016.9	15.248	0.995	1.2014	14.97
21	5696	794.4	3157.8	14.998	1.025	1.203	15.55
22	5857	836.56	3301.1	14.753	1.054	1.2048	16.11
23	6017	879.77	3447.1	14.512	1.082	1.2066	16.68

This page left intentionally blank.

TABLE A-2. Lithium Borohydride & Water

Working Fluid: Lithium Borohydride ($LiBH_4$) - 40% / Water (H_2O) - 60%

Electrical Energy Input kJ/g	Temperature K	Pressure MPa	Impetus J/g	Molecular Weight (-)	Covolume cm^3/g	Gamma (-)	Effective Energy kJ/g
0	1147	190.2	657	4.695	1.279	1.3138	2.09
1	1427.	220.06	818.0	4.719	1.283	1.2926	2.8
2	1661.	258.13	959.6	5.098	1.283	1.2752	3.49
3	1811.	288.20	1072.3	6.273	1.279	1.2571	4.17
4	1872.	304.25	1129.7	7.169	1.287	1.2470	4.57
5	1966.	331.85	1235.7	9.007	1.276	1.2296	5.38
6	2039.	358.48	1339.5	10.915	1.263	1.2148	6.24
7	2244.	404.52	1493.7	11.280	1.307	1.2072	7.22
8	2433.	447.61	1646.6	11.304	1.321	1.2044	8.06
9	2572.	490.11	1791.7	11.355	1.344	1.2043	8.77
10	2682.	533.35	1935.1	11.425	1.372	1.2056	9.41
11	2863.	584.58	2094.2	11.367	1.418	1.2044	10.25
12	3045.	630.36	2249.7	11.255	1.431	1.2039	11.03
13	3210.	675.12	2398.9	11.127	1.447	1.2043	11.74
14	3363.	719.25	2543.9	10.992	1.463	1.2052	12.4
15	3510.	763.29	2687.4	10.858	1.479	1.2064	13.02
16	3656.	808.08	2832.7	10.731	1.494	1.2075	13.65
17	3808.	854.13	2982.4	10.615	1.508	1.2084	14.31

TABLE A-2 Cont. Lithium Borohydride & Water

Working Fluid: Lithium Borohydride ($LiBH_4$) - 40% / Water (H_2O) - 60%

Electrical Energy Input kJ/g	Temperature K	Pressure MPa	Impetus J/g	Molecular Weight (-)	Covolume cm^3/g	Gamma (-)	Effective Energy kJ/g
18	3968	901.97	3138.9	10.512	1.520	1.2090	15.02
19	4142	951.69	3303.3	10.426	1.529	1.2091	15.94
20	4331	1003.32	3476.4	10.358	1.535	1.2087	16.66
21	4534	1056.50	3657.3	10.308	1.538	1.2079	17.59
22	4797	1110.67	3843.8	10.272	1.539	1.2067	18.60
23	4971	1165.36	4034.0	10.245	1.538	1.2053	19.65
24	5197	1220.02	4225.7	10.226	1.536	1.2038	20.73
25	5424	1274.36	4417.3	10.210	1.534	1.2023	21.84

TABLE A-3. Titanium Hydride & Aluminum & Water

Working Fluid: Titanium Hydride (TiH_2) - 12.5% / Aluminum (Al) - 37.5% / Water (H_2O) - 50%

Electrical Energy Input kJ/g	Temperature K	Pressure MPa	Impetus J/g	Molecular Weight (-)	Covolume cm^3/g	Gamma (-)	Effective Energy kJ/g
0	3011.	176.17	757.3	3.383	0.701	1.2707	2.8
1	3423.	200.96	863.9	3.386	0.701	1.2628	3.29
2	3812.	225.44	968.5	3.430	0.704	1.2574	3.76
3	4162.	249.22	1069.0	3.599	0.710	1.2539	4.21
4	4465.	272.03	1164.6	3.966	0.719	1.2514	4.63
5	4725.	294.09	1256.1	4.504	0.729	1.2496	5.03

TABLE A-4. Octane & Hydrogen Peroxide

Working Fluid: Octane (C_8H_{18}) - 25% / Hydrogen Peroxide (H_2O_2) - 75%

Electrical Energy Input kJ/g	Temperature K	Pressure MPa	Impetus J/g	Molecular Weight (-)	Covolume cm^3/g	Gamma (-)	Effective Energy kJ/g
0	3017	375.85	1486.7	16.873	1.044	1.2348	6.33
1	3432	429.84	1694.5	16.841	1.058	1.2272	7.45
2	3818	481.28	1891.6	16.781	1.07	1.2223	8.50
3	4170	530.46	2078.1	16.685	1.082	1.2193	9.47
4	4491	577.97	2255.7	16.555	1.097	1.2177	10.36
5	4784	624.42	2426.6	16.393	1.114	1.2173	11.16
6	5054	670.36	2592.9	16.207	1.132	1.2176	11.91
7	5306	716.31	2756.9	16.002	1.151	1.2186	12.61
8	5543	762.52	2919.8	15.785	1.171	1.22	13.27
9	5770	809.32	3082.9	15.562	1.191	1.2217	13.90
10	5989	856.91	3247.1	15.335	1.211	1.2237	14.51

DISTRIBUTION LIST

No. of Copies	Organization
12	Commander Defense Technical Info Center ATTN: DTIC-DDA Cameron Station Alexandria, VA 22304-6145
1	Commander USA Concepts Analysis Agency ATTN: D. Hardison 8120 Woodmont Avenue Bethesda, MD 20014
1	HQDA (SARD -TR) Washington, DC 20310
1	Commander US Army War College ATTN: Library-FF229 Carlisle Barracks, PA 17013
1	Director US Army BMD Advanced Technology Center PO Box 1500 Huntsville, AL 35807
1	Chairman DOD Explosives Safety Board Room 856-C Hoffman Bldg 1 2461 Eisenhower Avenue Alexandria, VA 22331
1	Commander US Army Materiel Command ATTN: AMCDRA-ST 5001 Eisenhower Avenue Alexandria, VA 22333
1	Commander US Army Materiel Command ATTN: AMCDRA-ST 5001 Eisenhower Avenue Alexandria, VA 22333-0001
5	Project Manager Cannon Artillery Weapons System, ARDEC, AMCCOM ATTN: AMCPM-CW, F. Menke AMCPM-CWW AMCPM-CWS, M. Fisette AMCPM-CWA, R. DeKleine H. Hassmann Picatinny Arsenal, NJ 07806-5000
1	Project Manager Munitions Production Base Modernization and Expansion ATTN: AMCPM-PBM-E, L. Laibson Picatinny Arsenal, NJ 07806-5000
3	Project Manager Tank Main Armament System ATTN: AMCPM-TMA, K. Russell AMCPM-TMA-105 AMCPM-TMA-120 Picatinny Arsenal, NJ 07806-5000

DISTRIBUTION LIST

No. of Copies — Organization

1 Commander
US Army Watervliet Arsenal
ATTN: SARWV-RD, R. Thierry
Watervliet, NY 12189

22 Commander
Armament RD&E Center
US Army AMCCOM
ATTN: SMCAR-MSI
SMCAR-TDC
SMCAR-AE
SMCAR-AEE-B,
A. Beardell
D. Downs
S. Einstein
S. Westley
S. Bernstein
N. Baron
A. Bracuti
J. Rutkowski
L. Stiefel
B. Brodman
SMCAR-CCD,
D. Spring
SMCAR-AEE,
J. Lannon
SMCAR-AES,
S. Kaplowitz
SMCAR-CCS
SMCAR-CCH-T,
L. Rosendorf
SMCAR-CCH-V,
E. Fennell
SMCAR-FSA-T,
M. Salsbury
Picatinny Arsenal, NJ
07806-5000

1 Commander
US Army Laboratory Command
ATTN: AMSLC-TD
Adelphi, MD 20783-1145

No. of Copies — Organization

4 Commander
US AMCCOM
ATTN: SMCAR-ESP-L
AMSMC-IRC, G. Cowan
SMCAR-ESM(R),
W. Fortune
R. Zastrow
Rock Island, IL 61299-7300

1 Director
Benet Weapons Laboratory
Armament R&D Center
US Army AMCCOM
ATTN: SMCAR-LCB-TL
Watervliet, NY 12189

1 Commander
US Army Aviation Systems Cmd
ATTN: AMSAV-DACL
4300 Goodfellow Blvd
St. Louis, MO 63120

1 Commander
US Army TSARCOM
4300 Goodfellow Blvd
St. Louis, MO 63120

1 Director
US Army Aviation Research
and Technology Activity
Ames Research Center
Moffett Field, CA 94035-1099

1 Commander
ERADCOM Technical Library
ATTN: STET-L
Fort Monmouth, NJ 07703-5301

DISTRIBUTION LIST

No. of Copies	Organization
1	Commander US Army Harry Diamond Lab ATTN: DELHD-TA-L 2800 Powder Mill Road Adelphi, MD 20783
1	Commander US Army Missile Command ATTN: AMSMI-RD-CS-R (DOC) Redstone Arsenal, AL 35898-5241
1	Commandant US Army Aviation School ATTN: Aviation Agency Fort Rucker, AL 36360
1	Commander US Army Tank Automotive Cmd ATTN: AMSTA-DI Warren, MI 48090
1	Commander US Army Tank Automotive Cmd ATTN: AMSTA-CG Warren, MI 48090
1	Project Manager Improved TOW Vehicle US Army Tank Automotive Cmd ATTN: AMCPM-ITV Warren, MI 48090
1	Program Manager M1 Abrams Tank System ATTN: AMCPM-GMC-SA, T. Dean Warren, MI 48090

No. of Copies	Organization
1	Project Manager Fighting Vehicle Systems ATTN: AMCPM-FVS Warren, MI 48090
1	President USA Armor & Engineer Board ATTN: ATZK-AD-S Ft. Knox, KY 40121
1	Project Manager M-60 Tank Development ATTN: AMCPM-M60TD Warren, MI 48090
1	Director TRADOC Analysis Command ATTN: ATAA-SL White Sands Missile Range, NM 88002-5502
1	Director Requirements & Programs Directorate HQ, TRADOC Analysis Command ATTN: ATCD-MA/MAJ Williams Ft. Monroe, VA 23651-5143
1	Commander USA Materials Technology Lab Dyna East Corporation ATTN: Christine P. Brandt, Document Control 3132 Market Street Philadelphia, PA 19104-2855
1	Commander US Army Research Office ATTN: Tech Library PO Box 12211 Research Triangle Park, NC 27709-2211

DISTRIBUTION LIST

No. of Copies	Organization
1	Commander US Army Belvoir R&D Ctr ATTN: STRBE-WC Tech Library (Vault) Bldg 315 Ft. Belvoir, VA 22060-5606
1	Commander US Army Logistics Ctr Defense Logistics Studies Ft. Lee, VA 23801
1	Commandant US Army Infantry School ATTN: ATSH-CD-CSO-OR Ft. Benning, GA 31905
1	President US Army Artillery Board Ft. Sill, OK 73503
1	Commandant US Army Command and General Staff College Ft. Leavenworth, KS 66027-5200
1	Commandant USA Special Warfare School ATTN: Rev & Tng Lit Div Ft. Bragg, NC 28307
1	Commander Radford Army Ammo Plant ATTN: SMCRA-QA/HI LIB Radford, VA 24141
1	Commander US Army Foreign Science & Technology Center ATTN: AMXST-MC-3 220 Seventh Street, NE Charlottesville, VA 22901
1	Commandant US Army Field Artillery Center & School ATTN: ATSF-CO-MW, B. Willis Ft. Sill, OK 73503
1	Office of Naval Research ATTN: Code 473, R.S. Miller 800 N. Quincy Street Arlington, VA 22217
2	Commander Naval Sea Systems Command ATTN: SEA 62R SEA 64 Washington, DC 20362-5101
1	Commander Naval Air Systems Command ATTN: AIR-954-Tech Lib Washington, DC 20360
1	Assistant Secretary of the Navy (R, E, and S) ATTN: R. Reichenbach Room 5E787 Pentagon Bldg Washington, DC 20350
1	Naval Research Lab Tech Library Washington, DC 20375
2	Commander US Naval Surface Weapons Ctr ATTN: J.P. Consaga C. Gotzmer Silver Spring, MD 20902-5000
3	Naval Surface Weapons Center ATTN: S. Jacobs/R10 Code 730 K. Kim/Code R-13 R. Bernecker/Code R-13 Silver Spring, MD 20902-5000

DISTRIBUTION LIST

No. of Copies	Organization
5	Commander Naval Surface Weapons Center ATTN: Code G33, J.L. East W. Burrell J. Johndrow Code G23, D. McClure Code DX-21 Tech Lib Dahlgren, VA 22448-5000
2	Commander Naval Underwater Systems Ctr Energy Conversion Dept ATTN: Code 5B331, R.S. Lazar Tech Library Newport, RI 02840
1	Commander Naval Weapons Center ATTN: Code 388, C.F. Price Info Science Div China Lake, CA 93555-6001
1	Superintendent Naval Postgraduate School Dept of Mechanical Engr Code 1424 Library Monterey, CA 93943
1	Program Manager AFOSR Directorate of Aerospace Sciences ATTN: L.H. Caveny Bolling AFB, DC 20332
3	Commander Naval Ordnance Station ATTN: D. Brooks W. Vienne Tech Library Indian Head, MD 20640
1	HQ AFSC/SDOA Andrews AFB, MD 20334
1	AFRPL/DY, Stop 24 ATTN: J.N. Levine/DYCR Edwards AFB, CA 93523-5000
1	AFRPL/TSTL (Tech Library) Stop 24 Edwards AFB, CA 93523-5000
1	AFRPL/MKPB, Stop 24 ATTN: B. Goshgarian Edwards AFB, CA 93523-5000
1	AFFTC ATTN: SSD-Tech Lib Edwards AFB, CA 93523
1	AFATL/DLYV ATTN: George C. Crews Eglin AFB, FL 32542-5000
1	AFATL/DLJE Eglin AFB, FL 32542-5000
1	Air Force Armament Lab ATTN: AFATL/DLODL Eglin AFB, FL 32542-5000
1	AFWL/SUL Kirtland AFB, NM 87117
1	Commandant USAFAS ATTN: STSF-TSM-CN Ft. Sill, OK 73503-5600
10	Central Intelligence Agency Office of Central Reference Dissemination Branch Room GE-47 HQS Washington, DC 20502
1	Central Intelligence Agency ATTN: Joseph E. Backofen HQ Room 5F22 Washington, DC 20505

DISTRIBUTION LIST

No. of Copies	Organization
2	Aeroject Solid Propulsion Co ATTN: P. Micheli P. Krshner Sacramento, CA 95813
1	ARMTEC ATTN: D. Simpson 85-901 Avenue 53 Coachella, CA 92236
1	Atlantic Research Corporation ATTN: M.K. King 5390 Cheorokee Avenue Alexandria, VA 22314
1	AVCO Everett Rsch Lab ATTN: D. Stickler 2385 Revere Beach Parkway Everett, MA 02149
1	Calspan Corporation ATTN: Tech Library PO Box 400 Buffalo, N 14225
1	FMC Corporation ATTN: Dr. G. Chryssomallis 1300 South Second Street PO Box 59043 Minneapolis, MN 55459-0043
1	GT Devices ATTN: Dr. S. Goldstein 5705A General Washington Dr Alexandria, BA 22312
1	General Electric Company Armament Systems Dept ATTN: M.J. Bulman, R-1311 Lakeside Avenue Burlington, VT 05401
1	Honeywell Inc. ATTN: R.E. Tompkins MN38-3300 10400 Yellow Circle Drive Minnetonka, MN 55343
1	IITRI ATTN: M.J. Klein 10W. 35th Street Chicago, Il 60616
1	Hercules, Inc Bacchus Works ATTN: K.P. McCarty PO Box 98 Magna, UT 84044
2	Director Lawrence Livermore National Laboratory ATTN: M.S. L-355, A. Buckingham PO Box 808 Livermore, CA 94550
1	Lawrence Livermore National Laboratory ATTN: M.S. L-355 M. Finger PO Box 808 Livermore, CA 94550
1	Olin Corporation Badger Army Ammunition Plant ATTN: R.J. Thiede Baraboo, WI 53913
2	Olin Corp/Smokeless Powder Operations R&D Library ATTN: V. McDonald Don Mann PO Box 222 St. Marks, FL 32355

DISTRIBUTION LIST

No. of Copies	Organization
1	Paul Gough Associates, Inc. ATTN: P.S. Gough PO Box 1614 1048 South St. Portsmouth, NH 03801
1	Physics International Company ATTN: Library H. Wayne Wampler 2700 Merced Street San Leandro, CA 94577
2	Rockwell International Rocketdyne Division ATTN: BA08 J.E. Flanagan J. Gray 6633 Canoga Avenue Canoga Park, CA 91304
1	Princeton Combustion Rsch Lab ATTN: M. Summerfield 4275 US Highway One Monmouth Junction, NJ 08852
1	Science Applications, Inc. ATTN: R.B. Edelman 23146 Cumorah Crest Woodland Hills, CA 91364
3	Thiokol Corporation Huntsville Division ATTN: D. Flanigan R. Glick Tech Library Huntsville, AL 35807
1	Scientific Rsch Assoc, Inc ATTN: H. McDonald PO Box 498 Glastonbury, CT 06033
1	Thiokol Corporation Wasatch Division ATTN: Tech Library PO Box 524 Brigham City, UT 84302
2	Thiokol Corporation Elkton Division ATTN: R. Biddle Tech Library PO Box 241 Elkton, MD 21921
1	Universal Propulsion Company ATTN: H.J. McSpadden Black Canyon Stage 1 Box 1140 Phoenix, AZ 85029
1	Veritay Technology, Inc. 4845 Millersport Hwy PO Box 305 East Amherst, NY 14051-0305
1	Battelle Memorial Institute ATTN: Tech Library 505 King Avenue Columbus, OH 43201
1	Brigham Young University Dept of Chemical Engr ATTN: M. Beckstead Provo, UT 84601
1	California Institute of Tech 204 Karman Lab Main Stop 301-46 ATTN: F.E.C. Culick 1201 E. California Street Pasadena, CA 91109

DISTRIBUTION LIST

No. of Copies	Organization
1	California Institute of Tech Jet Propulsion Laboratory ATTN: L.D. Strand 4800 Oak Grove Drive Pasadena, CA 91103
1	Professor Herman Krier Dept of Mech/Indust Engr University of Illinois 144 MEB; 1206 N. Green St Urbana, IL 61801
1	University of Minnesota Dept of Mechanical Engr ATTN: E. Fletcher Minneapolis, MN 55455
1	Washington State University Dept of Mechanical Engr ATTN: C.T. Crowe Pullman, WA 99163
1	Case Western Reserve U. Division of Aerospace Sciences ATTN: J. Tien Cleveland, OH 44135
3	Georgia Institute of Tech School of Aerospace Engr ATTN: B.T. Zinn E. Price W.C. Strahle Atlanta, GA 30332
1	Institute of Gas Technology ATTN: D. Gidaspow 3424 S. State Street Chicago, IL 60616
1	Johns Hopkins University Applied Physics Laboratory Chemical Propulsion Information Agency ATTN: T. Christian Johns Hopkins Road Laurel, MD 20707
1	Massachusetts Institute of Technology Dept of Mechanical Engr ATTN: T. Toong 77 Massachusetts Avenue Cambridge, MA 02139
1	Pennsylvania State Univ. Dept of Mechanical Engr ATTN: K. Kuo University Park, PA 16802
1	University of Michigan Gas Dynamics Lab Aerospace Engr Bldg ATTN: Dr. G.M. Faeth Ann Harbor, MI 48109-2140
1	Purdue University School of Mechanical Engr ATTN: J.R. Osborn TSPC Chaffee Hall West Lafayette, IN 47906
1	SRI International Propulsion Sciences Division ATTN: Tech Library 333 Ravenswood Avenue Menlo Park, CA 94025
1	Rensselaer Polytechnic Inst. Department of Mathematics Troy, NY 12181

DISTRIBUTION LIST

No. of Copies — Organization

1 Director
Los Alamos National Lab
ATTN: M. Division, B. Craig
T-3 MS B216
Los Alamos, NM 87545

1 Stevens Inst. of Tech
Davidson Laboratory
ATTN: R. McAlevy, III
Castle Point Station
Hoboken, NJ 07030

1 Rutgers University
Dept of Mechanical and
Aerospace Engr
ATTN: S. Temkin
University Heights Campus
New Brunswick, NJ 08903

1 U. of Southern California
Mechanical Engr Dept
ATTN: OHE200, M. Gerstein
Los Angeles, CA 90007

2 University of Utah
Dept of Chemical Engineering
ATTN: A. Baer
G. Flandro
Salt Lake City, UT 84112

No. of Copies — Organization

Aberdeen Proving Ground

Dir, USAMSAA
ATTN: AMXSY-D
AMXSY-MP, H. Cohen

Cdr, USATECOM
ATTN: AMSTE-TO-F

Cdr, CRDEC, AMCCOM
ATTN: SMCCR-RSP-A
SMCCR-MU
SMCCR-SPS-IL

Cdr, USACSTA
ATTN: S. Walton
G. Rice
D. Lacey
C. Herud

Dir, HEL
ATTN: J. Weisz

USER EVALUATION SHEET/CHANGE OF ADDRESS

This laboratory undertakes a continuing effort to improve the quality of the reports it publishes. Your comments/answers below will aid us in our efforts.

1. Does this report satisfy a need? (Comment on purpose, related project, or other area of interest for which the report will be used.) ____________________
2. How, specifically, is the report being used? (Information source, design data, procedure, source of ideas, etc.) ____________________
3. Has the information in this report led to any quantitative savings as far as man-hours or dollars saved, operating costs avoided, or efficiencies achieved, etc? If so, please elaborate. ____________________
4. General Comments. What do you think should be changed to improve future reports? (Indicate changes to organization, technical content, format, etc.) ____________________

BRL Report Number ____________ Division Symbol ____________

Check here if desire to be removed from distribution list. ____

Check here for address change. ____

Current address: Organization ____________________
Address ____________________

-----FOLD AND TAPE CLOSED-----

Director
U.S. Army Ballistic Research Laboratory
ATTN: SLCBR-DD-T(NEI)
Aberdeen Proving Ground, MD 21005-5066

OFFICIAL BUSINESS
PENALTY FOR PRIVATE USE $300

NO POSTAGE
NECESSARY
IF MAILED
IN THE
UNITED STATES

BUSINESS REPLY LABEL
FIRST CLASS PERMIT NO. 12062 WASHINGTON D.C.

POSTAGE WILL BE PAID BY DEPARTMENT OF THE ARMY

Director
U.S. Army Ballistic Research Laboratory
ATTN: SLCBR-DD-T(NEI)
Aberdeen Proving Ground, MD 21005-9989